Design of cantilever timber pole walls in cohesive soil

By

Kiwan Park

Thesis
Submitted to Flinders University
for the degree of

Master of Civil Engineering

College of science and engineering
12/12/2023

TABLE OF CONTENTS

ABSTRACT

The p-y curve is a graph that represents the relationship between soil resistance and the lateral displacement of a pile below the ground surface when the pile is subject to lateral loads. Numerous geotechnical engineering researchers have developed p-y curves for various environments and conditions. These curves have been designed for individual piles and pile groups in both offshore and onshore platforms. However, despite their wide use in New Zealand, cantilever timber pole walls, which are composed of timber poles, lack a dedicated p-y curve. Typically, the design of these timber pole walls in consulting firms has relied on the inaccurate continuous wall method. This method, which assumes the wall to be a single entity, fails to fully consider soil-pile interactions, such as the pile group reduction effect. Hence, this thesis aims to plot p-y curves for timber pole walls, taking into account the pile group reduction effect. The project involved creating new p-y curves for timber pole walls by utilising two analytical methods varying in strength and pile spacing. The conditions and environments for plotting these new curves are aligned with real-world scenarios for timber pole walls. These newly plotted p-y curves were compared with those generated by the RSPile software.

DECLARATION

I certify that this thesis:

1. does not incorporate without acknowledgment any material previously submitted for a degree or diploma in any university
2. and the research within will not be submitted for any other future degree or diploma without the permission of Flinders University; and
3. to the best of my knowledge and belief, does not contain any material previously published or written by another person except where due reference is made in the text.

Signature of student.....

Print name of student.....Kiwan Park.....

Date.....16/10/2023.....

I certify that I have read this thesis. In my opinion it is/is not (please circle) fully adequate, in scope and in quality, as a thesis for the degree of Master of Civil Engineering. Furthermore, I confirm that I have provided feedback on this thesis and the student has implemented it minimally/partially/fully (please circle).

Signature of Principal Supervisor.....

Print name of Principal Supervisor.....Hongyu Qin.....

Date... 16/10/2023.....

ACKNOWLEDGEMENTS

Firstly, I would like to express my deepest gratitude to my supervisor Dr. Hongyu Qin for his guidance on my thesis project and for his feedback throughout the project period. Specifically in moments when I encountered uncertainties in my thesis, he helped to guide me in the right direction. Additionally, the valuable resources provided by my supervisor were instrumental in enabling me to complete this thesis. Hence, I truly learned and gained a significant amount of knowledge and insight regarding pile structures thanks to this project.

I am also grateful to Prof. Rocco Zito, Prof. Adrian Werner, Dr. Thomas Vincent, Dr. Nicoholas Holyoak, and Research Associate Mr. Branko Stazic, from whom I have learned extensively about all four civil engineering disciplines while undertaking this degree.

Lastly, I would like to thank my family for their unwavering and consistent support throughout my entire degree. Also, I extend my thanks to my fellow students at Flinders University and friends from my home country for their valuable and heartfelt support, for which I am deeply grateful.

LIST OF FIGURES

LIST OF TABLES

1 INTRODUCTION

The retaining wall, a well-known geotechnical structure, is built to withstand the earth pressure, and it is also one of the most used type of retaining structures (Diwalkar, 2020). Retaining walls are employed in residential construction projects and large-scale infrastructure projects such as highways, railways, bridges, and irrigation sectors (Patil & Amir, 2015).

Recent global climate changes, resulting in increased landslides worldwide, have raised awareness of the importance of retaining structures' stability (Merzdorf, 2020). Common types of retaining walls include gravity-type walls, cantilever walls, and counterfort walls, which prevent sliding, overturning, and soil erosion from rain (Dhir, et al., 2017). The construction materials for retaining walls often consists of concrete, brick, or wood, depending on the site condition and the required construction type (Diwalkar, 2020). Due to its cost-effectiveness compared to concrete and brick, timber-based retaining walls are widely constructed worldwide. Specifically, wood retaining walls cost about $19 per square foot, while I-beam retaining walls range from $35 to $150 per square foot. (Wallender, et al., 2023). Moreover, wood retaining walls tend to have a lengthy lifespan of at least 20 years (Versace Timbers, 2023). In New Zealand, cantilever timber pole walls, are widely utilised in both residential and large-scale infrastructure projects due to their affordability and longevity (Wood, 2021).

In the design of laterally loaded timber pole retaining walls, geotechnical engineers typically use the continuous wall method (Georgiadis, 2018). This method assumes the timber pole wall to be a single entity with two-dimensional design approach (Georgiadis, 2018). More specifically, the continuous wall method applies equivalent stiffness throughout the design process, differing from the actual specification of soldier pile walls and timber pole walls, which consist of timber poles and timber railway sleepers between them (Georgiadis, 2018). The simplicity of the continuous wall method makes it popular in consulting firms since the continuous wall method is based on the assumption of the row of piles as a one single wall (Georgiadis, 2018). However, this approach does not account for soil-pile interaction between the poles of the wall such as the pile group reduction effect of the piled walls, leading to inaccurate designs.

2 LITERATURE REVIEW

2.1 Background

2.1.1 Cantilever Timber Pole Wall

According to Wood (2021), typical heights for cantilever timber pole walls range from 1.5 m to a maximum of 3.5 m. In addition, the diameter of the timber poles is between 0.4 m and 0.6 m, with the height of the wall is almost equal to the embedment depth of the wall (Wood, 2021). Walls with a height of over 3.5 m require adequate stability features, such as grouted tiebacks. However, this thesis focuses on walls of low to moderate height, specifically walls equal or below the height of 2 m.

In terms of materials, the backfill region of the wall generally consists of free-flowing materials like sand, gravel, and geotextile, which aid drainage during the wet season (Timber Queensland, 2014). Below the ground surface, cohesive soil types such as clay are utilised for this project. Clayey soil, known for causing geotechnical engineering challenges due to its chemical and physical properties, tends to shrink and swell in response to changes in moisture content and climate cycles (Yalcin, 2007; Medjnoun & Bahar, 2016). The clayey soils shrink and swell according to the change of moisture content and climate cycle (Medjnoun & Bahar, 2016). Particularly, the swelling nature of clayey soil, influenced by moisture and seasonal weather, has caused damage to lightweight structures worldwide (Medjnoun & Bahar, 2016; Jaska, 1992). Moreover, the majority of the Adelaide region is underlain by expansive clays, such as Hindmarsh clays, which have historically presented challenges for various structures (Jaska, 1992). Figure 1 and Figure 2 are the cantilever pole walls taken from Wood (2021).

Figure removed due to copyright restriction

Figure 1: Cross-section of the wall **(Wood, 2021)**

Figure removed due to copyright restriction

Figure 2: The cantilever timber pole wall **(Wood, 2021)**

As shown in Figure 1, the pole of the wall is driven approximately 2 meters into the ground. The embedded part of the timber pole constitutes the wall portion, which resists lateral pressure from the backfill region.

2.1.2 The p-y Curve Method

Structures supported by piles are frequently influenced by horizontal forces from various sources such as traffic, wind, and seismic activities (Higgins, et al., 2013). In designing process of the pile or pole structures, the p-y curve method is globally utilised for achieving the lateral load capacity of the pile structure and is the most efficient method (Suryasentana & Lehane, 2016). In this method, the pile is assumed as a series of beam elements, and the soil is expressed as the non-linear springs along the pile's embedded length below the ground surface (Lehane, et al., 2022). Figure 3 shows the pile under lateral loading taken from (Reese & Van Impe, 2009).

Figure removed due to copyright restriction

Figure 3: Pile under lateral loading **(Reese & Van Impe, 2009)**

The p in the p-y curve signifies the soil resistance per unit length along the pile, while the y symbol indicates the lateral displacement when the load is applied to the pile (Reese & Van Impe, 2009). Specifically, when exerting the horizontal load on the pile head, the pile shows lateral displacement and squeezes the soil on the side of the pile, so the soil surrounding the pile results in reaction force to prevent further deformation (Kong, et al., 2020).

2.1.3 Existing P-y Curve Method for Individual Pile (Matlock Method)

For the pile in the soft clay environment, Matlock (1970) developed a p-y curve for individual pile employing a parabolic function (Terceros, et al., 2017). Soft clay is located near or under the water table, where a significant amount portion of it is comprised of clayey material and silty material, which has high moisture content (Bergardo & Kamon, 1991). Matlock (1970) developed the p-y curves for piles on soft clay based on the data results of four laterally loaded pile tests in Texas that were designed for offshore conditions (Steven, 1988). The steel-pipe pile with a diameter of 12.75 inches and 42 feet in length was utilized for the test.

$$y_{50} = 2.5\varepsilon_{50}b \qquad \text{Equation 1}$$

y_{50} is the lateral displacement at one-half of the ultimate resistance. (Wang & Sitar, 2006). b is the diameter of the pile (Wang & Sitar, 2006). Where ε_{50} represents the normal strain value, which corresponds to one-half of the maximum principal stress difference in the triaxial test, and b signifies the diameter of the pile (Wang & Briaud, 2018). $\varepsilon_{50}$is derived from the soil data of clayey material, including both in-situ and laboratory test results (Ebrahimian & Nazari, 2014). The ultimate lateral load of the pile increases at higher values of pile lateral displacements as ε_{50} increases. Consequently, ε_{50} influences both the stiffness of the soil and the soil resistance around the pile (Ebrahimian & Nazari, 2014). In other words, ε_{50} is considered essential in the p-y curve plotting process, as it helps identify the stiffness of the stress-strain curves (Reese & Van Impe, 2009). Table 1 presents ε_{50} values for stiff to soft clay, as reported by Rocscience (2018).

Table 1: Value of normal strain for the clay **(Ishenhower & Wang, 2016) (Rocscience, 2018)**

Consistency of Clay	Normal Strain Value (ε_{50})
Soft	0.02
Medium	0.01
Stiff	0.005

The value of p can be determined by using Equation 2.

$$p = \frac{p_u}{2}\left(\frac{y}{y_{50}}\right)^{1/3} \qquad \text{Equation 2}$$

P_u is the soil ultimate lateral resistance (Wang & Sitar, 2006). P_u can be calculated using conservative value resulting from Equation 3 and Equation 4.

$$P_u = 9 \times S_u \times B \qquad \text{Equation 3}$$

$$P_u = \left(3 + \frac{r'_{avg}}{S_u}x + \frac{J}{B}x\right)S_u \times B \qquad \text{Equation 4}$$

Where

r'_{avg} = average effective unit weight

x = depth from the ground surface to the p-y curve

S_u= undrained shear strength(kPa)

B= The diameter of the pile

J= 0.5 for soft clay, dimensionless fitting coefficient

2.1.4 Existing p-y Curve Method for Individual Pile (Reese Method)

Reese and Welch (1975) developed the p-y curve for an individual pile in a stiff clay environment above the water table, based on data from one full-scale, field laterally loaded pile test (Steven, 1988). To collect and plot the test results, a 10.75-inch-diameter circular pipe was positioned below the ground surface. This actual pile test led to the development of equations for computing the p-y curve, as outlined in Equation 5 (Steven, 1988).

$$y_{50} = 2.5\varepsilon_{50}b$$

$$P = \frac{p_u}{2}\left(\frac{y}{y_{50}}\right)^{1/4} \quad \text{Equation 5}$$

P_u is the soil ultimate lateral resistance (Wang & Sitar, 2006). P_u can be calculated using conservative value resulting from Equation 3 and Equation 4.

2.2 Approach for plotting the new p-y curve of the timber pole wall

2.2.1 Georgiadis Method For Ultimate Lateral Soil Resistance In Soldier Pile Wall

The ultimate soil lateral resistance (P_u) depends on lateral bearing capacity factor, undrained shear strength, and pile diameter, which can be calculated using Equation 6 (Wang & Briaud, 2018). The ultimate soil lateral resistance signifies the maximum soil lateral resistance around the pile below the ground surface when the pile is loaded by lateral force.

$$P_u = N_p S_u B \quad \text{Equation 6}$$

Where N_p is the bearing capacity factor, S_u is the undrained shear strength of clay, and B is the pile diameter. Figure 4 displays the front view of the soldier pile wall taken from Georgiadis (2018).

Figure removed due to copyright restriction

Figure 4: Soldier pile wall **(Georgiadis, 2018)**

Figure 4 shows the cross-section of the soldier pile wall, indicating variables of the soldier pile wall, such as the pile embedment length below the ground as 'L' as well as 'H' for the height of the wall above the excavated surface. However, on the numerical modelling process for this project, 'L' signifies the total pile length and 'H' represents the wall height above the excavated surface (Georgiadis, 2018). Since the soldier pile wall consists of a group of piles which support the pressure of the backfill region, Georgiadis (2018) developed a method for achieving the soil lateral bearing capacity factor for the pile below the ground surface under such condition. Particularly, the method that was devised by Georgiadis (2018) is based on the result of 3D finite-element analysis utilizing Plaxis 3D Foundation (Georgiadis, 2018). The type of the wall on the 3D software analysis was soldier pile wall which is different to the timber pole wall in terms of the pile material and the height of the wall. Additionally, the soldier pile wall is successfully utilized without any issues in the excavation work deeper than 30 m whereas timber pole wall is suitable for the low height excavation work which is from 1.5 m to 3.5 m. (Perko, 2008). However, although there are some differences between the soldier pile wall and the timber pole wall, since the engineering principle is same on both retaining walls, Georgiadis (2018) method is employed for this project for calculation of the soil lateral resistance of the timber pole wall. The adequate portion of the Georgiadis (2018) method that is suitable for timber pole wall will be summarized and employed. Figure 5 shows the rotation point of the pile taken from Wang et al (2022).

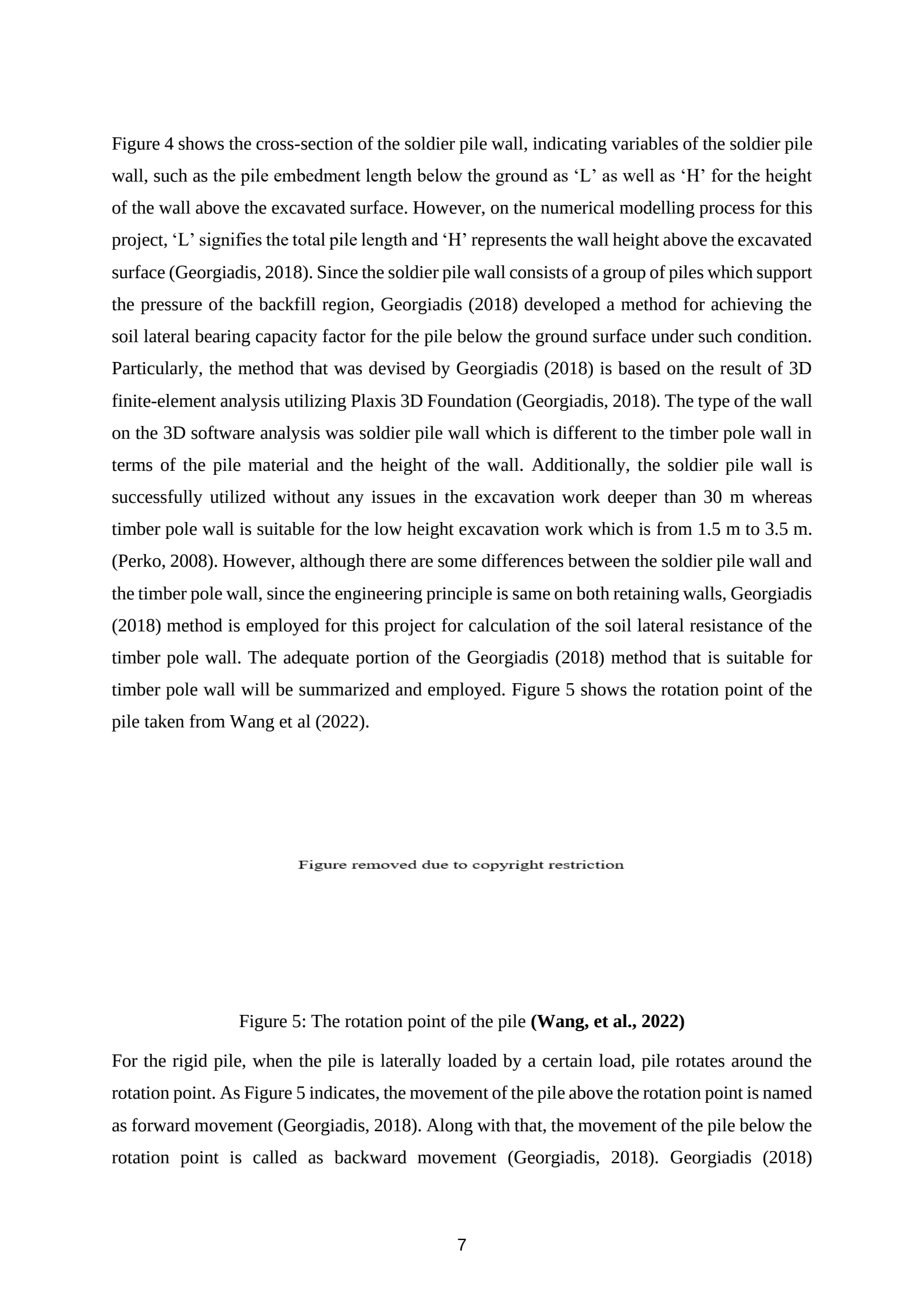

Figure 5: The rotation point of the pile **(Wang, et al., 2022)**

For the rigid pile, when the pile is laterally loaded by a certain load, pile rotates around the rotation point. As Figure 5 indicates, the movement of the pile above the rotation point is named as forward movement (Georgiadis, 2018). Along with that, the movement of the pile below the rotation point is called as backward movement (Georgiadis, 2018). Georgiadis (2018)

developed analytical equations for the calculation of the lateral bearing capacity factor depending on these two movements as well as the weight of the surcharge load of the backfill region. Once the ultimate soil lateral bearing capacity factor (N_p) is obtained by the Georgiadis method, the maximum soil resistance is directly calculated using Equation 6. For this project, the pile group reduction effect which is present to the group of piles is mainly analyzed. In this project, the words 'pile' and 'pole' mean the same entity, which is timber pole.

2.2.2 Motta Method for Lateral Displacement in Cohesive Soil

With respect to the analytical calculation of the pile lateral displacement in the p-y curve, the Motta method is selected as this method is developed for the displacement analysis of the pile, especially in cohesive soil. Regarding the process of resulting the lateral displacement, once the ultimate soil lateral resistance around the pile is specified by Georgiadis (2018) method, the lateral displacement can be specified utilizing the Motta method in the dimensionless form. To be more specific about the dimension of the displacement, the displacement that resulted from the Motta method does not have any dimensions such as centimetres and millimetres. Specifically, Motta (2013) classified the soil reaction state around the pile below the ground surface into three cases regarding the strength of the horizontal force that acts on the pile head. The lateral load and the moment for this method were indicated as dimensionless forms by Equations 7 and 8.

$$h = \frac{H_0}{P_{lim} L} \qquad \text{Equation 7}$$

$$m = \frac{M_0}{P_{lim} L^2} \qquad \text{Equation 8}$$

where P_{lim}=limiting lateral load (Motta, 2013).

h= dimensionless force

m= dimensionless moment

Since the load and the moment is dimensionless, the lateral displacement of the pile head that resulted from the Motta method is also resulted in dimensionless form.

Case 1: The horizontal force that acts on the pile head is small that the pile displacement will be less than the limit displacement value and the interaction between soil and the pile (Motta, 2013). Figure 6 illustrates the case 1 of the pile.

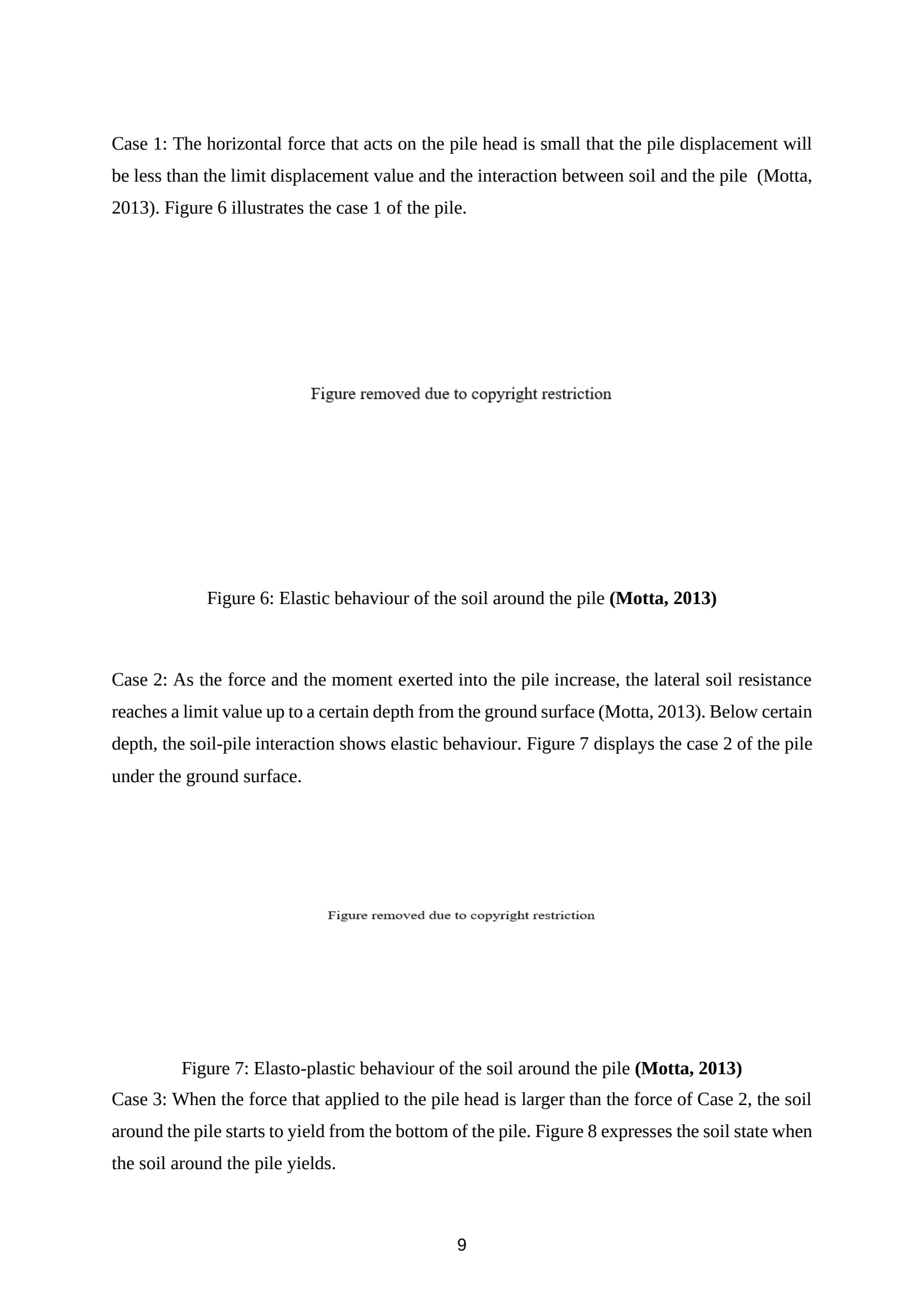

Figure 6: Elastic behaviour of the soil around the pile **(Motta, 2013)**

Case 2: As the force and the moment exerted into the pile increase, the lateral soil resistance reaches a limit value up to a certain depth from the ground surface (Motta, 2013). Below certain depth, the soil-pile interaction shows elastic behaviour. Figure 7 displays the case 2 of the pile under the ground surface.

Figure 7: Elasto-plastic behaviour of the soil around the pile **(Motta, 2013)**

Case 3: When the force that applied to the pile head is larger than the force of Case 2, the soil around the pile starts to yield from the bottom of the pile. Figure 8 expresses the soil state when the soil around the pile yields.

Figure 8: Soil yielding from the bottom of the pile **(Motta, 2013)**

2.3 Pile Group Reduction Factor

When the piles are installed in a group below the surface ground, the soil-pile interaction between the piles incurs the reduction of the lateral resistance of each pile (Fayyazi, et al., 2014). The pile group reduction factor is also referred to as the p-multiplier or pile spacing effect and is dependent on the normalised pile spacing, which is S/D (Rollins, et al., 2006). S is the value of pile spacing, and D signifies the diameter of the pile. More specifically, since each pile in a group of piles influences to the soil resistance around the piles, the sum of lateral resistance of individual piles shows greater value than the lateral resistance of the pile group (Fayyazi, et al., 2012). Figure 9 shows the pile group reduction effect in terms of lateral soil resistance taken from Fayyazi et al (2012).

Figure 9: Pile group reduction effect **(Fayyazi, et al., 2012)**

Figure 9 represents the pile group reduction effect where there is different horizontal soil resistance between single pile and a pile in a pile group (Fayyazi, et al., 2012). The p-multiplier which is pile group reduction factor is dependent on the row spacing of the pile groups (Fayyazi, et al., 2012). Georgiadis et al (2013) performed the finite element analysis of pile-soil interaction in terms of different pile spacing and established the equation that can result in the p-multipliers on various pile spacings. The p-multiplier turned out to be related to the

normalised pile spacings, which is $\frac{S_1}{D}$. To explain the terminology of $\frac{S_1}{D}$, $S_1$is the value above which the group effect starts to diminish (Georgiadis, 2018).

The equations of p-multiplier, critical spacing, and pile-soil adhesion factor can be expressed as the following equations:

$$f_{mug} = \frac{N_{pug}}{N_{pu1}} = 1 + \left(0.13 ln \frac{\frac{s}{D} - 1}{\frac{S_1}{D} - 1} + 0.24 - 0.02\alpha \right) ln \frac{\frac{s}{D} - 1}{\frac{S_1}{D} - 1} \quad \text{Equation 9}$$

$$\frac{S_1}{D} = 3.1 + 1.4\alpha \quad \text{Equation 10}$$

$$\alpha = 0.21 + \frac{26}{s_u} \leq 1 \ (S_u \ in \ kPa) \quad \text{Equation 11}$$

$$N_{pu1} = \pi + 2arcsin\alpha + 2\cos(arcsin\alpha) + 4[\cos\left(\frac{arcsin\alpha}{2}\right) + \sin\left(\frac{arcsin\alpha}{2}\right)] \quad \text{Equation 12}$$

Where N_{pu1} is the ultimate bearing capacity factor and N_{pug} is the ultimate bearing capacity factor considering group effect (Georgiadis, 2018).The soil-pile adhesion factor is expressed as α and specify the ratio between the soil's cohesive and adhesive strength under various water content. (Chen & Broecke, 2021). With respect to the pile-soil adhesion factor (α), Kulhawy (1991) developed an equation where the pile-soil adhesion factor can be induced from undrained shear strength of the soil which can be seen in Equation 11.

2.4 The Continuous Wall Method and Pile Spacing

Georgiadis (2018) stated that the geotechnical engineering consulting firms normally employ the two-dimensional (2D) finite-element analysis for the design of solider pile walls which assumes the row of piles as a one single continuous wall. Since the continuous wall method is based on the assumption of the row of piles as a one single continuous wall, the pile group reduction effect which is dependent on the pile spacing could not be considered during the design process when the continuous wall method is utilized for design process. In other words, the pile spacing is not considered in the continuous wall method.

2.5 Research gap

Several researchers have developed the p-y curves to help geotechnical engineers accurately analyse and design pile structures in various environments. Prior to the development of the Matlock method, McClelland & Focht (1958) proposed the concept of p-y curves for clay soil in one of the first papers (Reese & Van Impe, 2009). From the work performed by McClelland & Focht (1958), the equations for p-y curves were developed based on a consolidated-undrained triaxial test. A few years later, Matlock (1970) finalized the development of the p-y curve for the pile in a soft clay environment, and Reese and Welch (1975) devised the p-y curve to predict the pile behaviour in terms of soil lateral resistance and lateral displacement in stiff clay platform. Additionally, Reese and Welch (1975) subclassified the p-y curve in a stiff clay environment where free water is present and free water is not present. Figure 10 is the p-y curve under static loading in stiff clay without free water taken from (Reese & Van Impe, 2009). Figure 11 shows the p-y curve for static loading in stiff clay in the presence of water taken from (Reese & Van Impe, 2009).

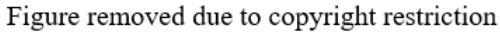

Figure 10: The p-y curve for static loading in stiff clay without free water **(Reese & Van Impe, 2009)**

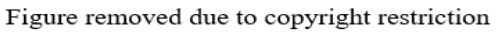

Figure 11: The p-y curve for static loading in stiff clay in the presence of free water **(Reese & Van Impe, 2009)**

Not only are there p-y curves for static loading, but also there are p-y curves for cyclic loading. Likewise, there are several p-y curves in different environments that researchers have developed. The p-y curves developed from previous researchers are based on individual pile. Even though numerous p-y curves have been developed for different environments (clay and sand) for individual pile, the p-y curve for the timber pole walls have not been plotted so far. Thus, the newly plotted p-y curves for timber pole walls will help geotechnical engineers to design the cantilever pole walls readily.

2.6 Research aim

The detailed objectives of the project could be analysed into three sub-sections.

1. Analysis of the lateral load-displacement curve in terms of different soil strength:

The analysis is performed in terms of different undrained shear strength. Typically, it is expected that the greater soil lateral resistance is resulted when the larger lateral load exerts to the pile. As a result, the newly plotted p-y curves are plotted and checked in terms of different soil strengths.

2. Analysis of the lateral load-displacement curve in terms of different pile-spacings:

Since the close-spacing of the piles affects the soil lateral resistance around the pile, it is expected that the wall that is composed of the closer pile spacing results on the relatively

smaller soil lateral resistance. The newly plotted p-y curves are also compared in terms of the different pile-spacings to check whether the curve shows the expected behaviour or not.

3. Comparison process of analytically plotted p-y curve with RSPile software:

After plotting the new p-y curves, the newly plotted p-y curves are compared with the p-y curves from numerical method which is RSPile software developed from Rocscience Inc. The soil parameters and test conditions of the numerical method, such as soil strength, pile diameter, the height of the wall and the embedded length of the pile are unified with analytical method.

3 METHODOLOGY

The methodology of this project is divided into analytical method and numerical method. The process and methods of the project are visualised by the flow diagram on the Figure 13. The newly plotted p-y curves are compared with the p-y curves that resulted from the Reese method and software analysis. Firstly, the p-y curves from numerical modeling which are based on RSPile software are compared to the p-y curves from the Reese method to judge the accuracy of the software numerical modeling. Secondly, the p-y curves from software analysis are utilized for comparison process with the newly plotted p-y curves for the final process. To be more specific about the p-y curves, the p-y curves for timber pole walls are plotted in terms of two different normalised pile spacings (S/D=2,4) and three different soil strengths (strength=50,100, and 200 kPa). In other words, six sets of p-y curves are made from analytical method as well as six sets of p-y curves from numerical method. Figure 12 illustrates the value of undrained shear strength according to the depth in Adelaide region taken from Jaksa & Kaggawa (1992).

Figure removed due to copyright restriction

Figure 12: The variation of undrained shear strength **(Jaksa & Kaggwa, 1992)**

With regards to clay material in Adelaide region, the predominant undrained shear strength value was determined referring to Figure 12. To be more specific about the undrained shear strength, the medium state of clay normally has the undrained shear strength of 50 kPa. (Abdul Karеam, et al., 2020). The stiff state of the clay is between 50 kPa and 100 kPa. Additionally, the very stiff clay generally has the undrained shear strength between 100 kPa and 200 kPa. Since this thesis project is mainly focused on the medium stiff clay ground where the timber pole wall is constructed, the undrained shear strength between 50 kPa and 200 kPa is selected. Table 2 shows the undrained shear strength according to soil consistency adapted from Ayadat (2021).

Table 2: The undrained shear strength of the clay **(Ayadat, 2021)**

Consistency	Undrained shear strength, C_u(kPa)	
	Vane Test	Swedish cone
Very Soft	<12	<7
Soft	12~25	7~19
Firm	25~50	19~42
Stiff	50~100	42~89
Very Stiff	100~200	89~193
Hard	>200	>193

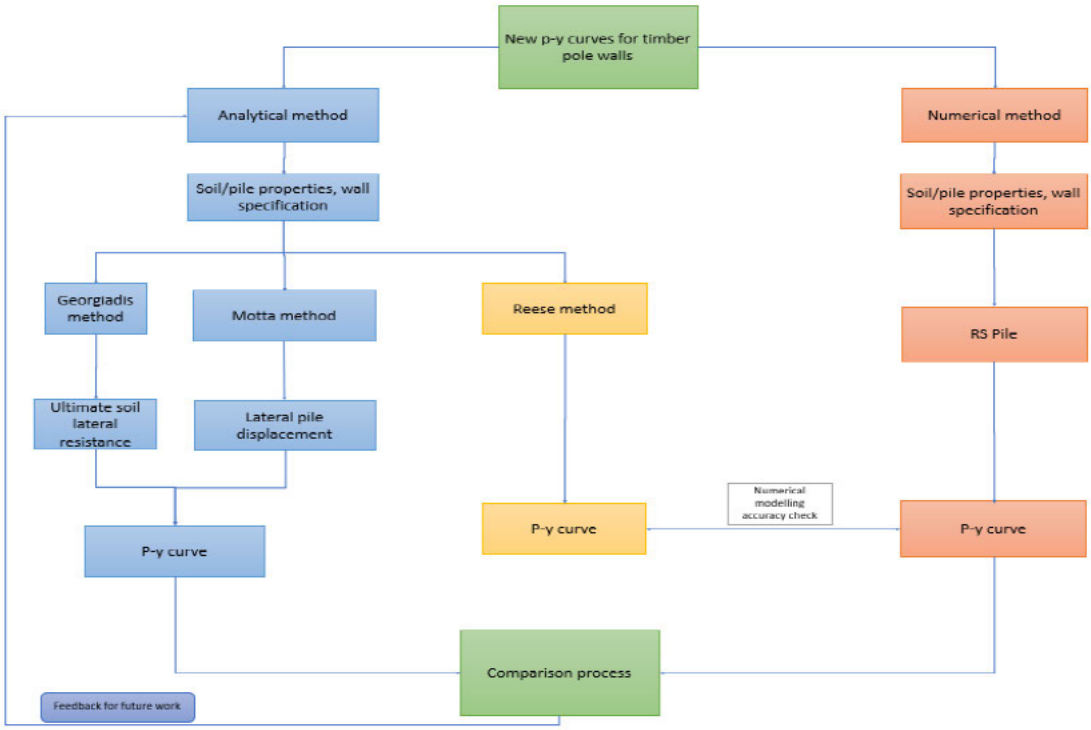

Figure 13: The methodology of the project

3.1 Analytical Method (Calculation process)

This chapter illustrates the one example of the analytical computation process for the ultimate lateral resistance and the lateral displacement by two analytical methods to show the specific analytical method process. All other results for other five cases will be explained in result and discussion chapter.

3.1.1 Maximum Pile Displacement Limit

The value of maximum lateral pile displacement was determined referring to previous studies. Georgiadis (1999) performed experimental tests to achieve the result of the lateral displacement of the cantilever sheet pile walls and the value of the maximum lateral displacement was around 50mm before pile structure failure (Georgiadis & Anagnostopoulo, 1999). To clearly plot the elasto-plastic behaviour of the timber pole onto the graph, the maximum timber pole head displacement is set as 200 mm for this thesis project.

3.1.2 Soil Lateral Resistance Resulting Process By Georgiadis Method (Analytical Method)

3.1.2.1 Timber Pole Wall Dimension And Soil Parameters For Analysis.

To achieve the value of soil lateral resistance around the timber pole below the ground surface when the timber pole is laterally loaded, several conditions and parameters are specified and assumed referring to the timber pole wall design resources before the actual analytically calculation process. Adhering to the actual specification of the cantilever timber pole walls in the real world, the wall height is set as 2 m for this project which is same with pole embedment length below the ground surface. Regarding the diameter of the pole, it is 500mm which is between 400 mm and 600 mm. The soil type of the backfill region behind the wall is specified as sand material whereas the soil type below the ground surface is the clay material which is cohesive soil. During the calculation process of the weight of the backfill region behind the wall, the weight of the backfill region is also be referred as the surcharge load. The specific details of the soil are explained by Table 3.

Table 3: Soil material

Material	Unit weight (kN/m^3)	Normal strain
Sand (dry)	16	N/A
Clay	18	0.01

Regarding the surcharge load of the backfill region, the surcharge load is expressed as $q = \gamma h$ (where γ is the bulk unit weight of the sand and h indicates the height of the pole above the ground level) (Georgiadis, 2018).

Table 4: Surcharge load

Surcharge load (q)	Wall height (m)	Sand unit weight (kN/m^3)	Surcharge load (kN/m^2)
	2	16	32

The surcharge load (q) is usually expressed with the undrained shear capacity (q_u) of the clay below the ground. When the surcharge load is expressed with the undrained shear capacity, the normalised surcharge load is q/q_u. Depending on the strength of the normalised surcharge load, the equation of the ultimate soil lateral bearing capacity is variable. However, since the wall height is specified as 2 m, the weight of the surcharge load is fixed to 32 kN/m^2 for this project. Regarding the specific detail of the normalised surcharge load, when the undrained shear strength is 50 kPa and the retaining wall height is 2 m, the normalised surcharge load is expressed as Equation 13. The normalised surcharge load is in dimensionless form.

$$q/q_u = \frac{32}{5.2 \times S_u} = 0.123 \qquad \text{Equation 13}$$

With respect to the pile spacings of the timber pole retaining wall, the pile spacing value is normally expressed as the normalised pile spacing (S/D). For instance, the pile spacing of the wall where the spacing is 1m and the diameter is 0.5m is expressed as S/D of 2.

3.1.2.2 Ultimate Soil Lateral Resistance Above The Rotation Point Of The Timber Pole Wall For 1 m Spacing, 500 mm Diameter And 50 kPa Strength Clay (Forward Movement)

The soil lateral resistance above the rotation point is the region where the pole leans toward to the excavated zone when the pole is laterally loaded. This portion of the pole usually takes up about 60%~70% of the total pole length embedded below the ground. Thus, for the forward movement of the pole, the embedded depth of 1.3 m below the ground surface is chosen for analytical p-y curve analysis. The normalised pole spacing for case 3.2.1 is S/D of 2. Before achieving the soil lateral resistance, the lateral bearing capacity factor should be resulted. For the clay that has 50 kPa undrained shear strength, the normalised surcharge load is expressed as Equation 13.

$$q/q_u = \frac{32}{5.2 \times S_u} = 0.123$$

For $q/q_u < 0.5$, the bearing capacity factor for a pile in group (forward movement) is

$$N_{pg} = N_{pzo} + 0.375 \frac{(z - z_o)}{D} \leq N_{pug} \quad \text{Equation 14}$$

Where N_{pzo} is the value of N_{p1} at z=z_o and N_{p1} is expressed as Equation 15

$$N_{p1} = N_{pu1} - \left(N_{pu1} - N_{po}\right) e^{-\lambda\left(\frac{z}{D}\right)} \quad \text{Equation 15}$$

To get the value of N_{pzo}, equation 11,12,16 and 17 are required.

$$\alpha = 0.21 + \frac{26}{s_u} = 0.21 + \frac{26}{50} = 0.73$$

$$N_{po} = 2 + 1.5\alpha = 3.095 \quad \text{Equation 16}$$

$$N_{pu1} = \pi + 2arcsin\alpha + 2\cos(arcsin\alpha) + 4[\cos\left(\frac{arcsin\alpha}{2}\right) + \sin\left(\frac{arcsin\alpha}{2}\right)] = 11.406$$

$$\frac{z_o}{D} = 0.1\left[\frac{(4.45 + 0.5\alpha)s}{D} - 1\right] = 0.863 \quad \text{Equation 17}$$

N_{po} is the bearing capacity at the ground surface (Georgiadis, 2018). The value of $\frac{z_o}{D}$ signifies the critical depth. The critical depth is the point where the bearing capacity factor of single pile (N_{p1}) deviates from the bearing capacity factor of a pile in a group (N_{pg}). The symbol of N_{pzo} is resulted as 5.721 using Equation 13. Finally, the bearing capacity factor for N_{pg} is 6.37 using Equation 14. As a result, the soil ultimate lateral resistance value when the normalised pile spacing is 2, the diameter of timber pole is 500 mm, and the clay strength is 50 kPa is resulted as following Equations:

3.1.2.3 Sample of Soil Ultimate Lateral Resistance Calculations

$$P_u = N_p S_u B = 6.37 \times 50 \times 0.5 = 159.308\ kN/m$$

$$f_{mug} = \frac{N_{pug}}{N_{pu1}} = 1 + \left(0.13 ln \frac{\frac{S}{D} - 1}{\frac{S_1}{D} - 1} + 0.24 - 0.02\alpha \right) ln \frac{\frac{S}{D} - 1}{\frac{S_1}{D} - 1}$$

$$= 0.912$$

$$P_u(considering\ group\ effect) = P_u * 0.912 \qquad \text{Equation 18}$$

$$= 145.3kN/m$$

3.1.3 Lateral Timber Pole Head Displacement By Motta Method (Analytical Method)

Figure removed due to copyright restriction

Figure 14: Elastic perfectly plastic curve **(Huang, et al., 2023)**

Figure 14 represents the illustrative graph of the elastic perfectly plastic curve where only elastic state and plastic state are present taken from Huang et al (2023). Specifically, when the soil reaches the yielding point where the soil around the pile below the ground surface yields, the lateral soil resistance of the curve does not change with increasing displacement. The trend of the new p-y curves will show similar trend with the graph in Figure 14.

Using the value of the ultimate soil lateral resistance that was resulted in section 3.1.2.3, the lateral pole displacement is calculated by Motta method. The ultimate soil lateral resistance is also expressed as limiting lateral load per length in Motta method (Motta, 2013). The lateral load that applies to the pole head increases until it reaches the ultimate soil lateral resistance.

Regarding the displacement, the value is achieved by the equations that correspond to the certain soil state depending on the lateral load. For the pile lateral displacement in case 1, the lateral displacement at the pile head for the case 1 is expressed as following equation:

$$y_L = \frac{y_h E_s}{P_{lim}} = 4h + 6m \leq 1 \qquad \text{Equation 19}$$

Regarding the pile lateral displacement in Case 2, the lateral displacement at the pile head for the case 2 is expressed as following equation:

$$y_L = 1 + \frac{4(1-h)^2(4h+6m-1)}{(3-6h-6m)^2} \qquad \text{Equation 20}$$

Case 2 occurs under following two conditions:

$$4h + 6m > 1 \qquad \text{Equation 21}$$

$$2h^2 + 2h + 6m \leq 1 \qquad \text{Equation 22}$$

Additionally, the lateral displacement at the pile head for the case 3 is expressed as following equation:

$$y_L = \frac{1+h}{\sqrt{3-3h^2-6h-12m}} \qquad \text{Equation 23}$$

Case 3 occurs under following two conditions:

$$2h^2 + 2h + 6m > 1 \qquad \text{Equation 24}$$

$$h^2 + 2h + 4m \leq 1 \qquad \text{Equation 25}$$

Apart from the displacement, the soil lateral resistance that is less than the ultimate soil lateral resistance is resulted by Equation 26 referring to the Motta method.

$$Soil\ lateral\ resistance\ (p) = \frac{4HL + 6M}{L^2} \qquad \text{Equation 26}$$

Where the symbol ‘H’ means the lateral load, ‘M’ signifies the moment, and ‘L’ represents the embedded length of the pole below the ground. For the visual explanation of the calculating the lateral displacement of the pole by Motta method, Table 5 is attached.

Table 5: The spreadsheet of soil lateral resistance and displacement combining Georgiadis method and Motta method.

Lateral load(kN)	Moment(kN*m	h(dimensionless load)	m(dimensionless moment)	Soil lateral resistance(kN/m)	Normalised Displacement
		H/Plim/L	M/Plim/L^2		
1	0.67	0.003	0.001	3	0.021
10	6.67	0.034	0.011	30	0.207
20	13.33	0.069	0.023	60	0.413
30	20.00	0.103	0.034	90	0.620
40	26.67	0.138	0.046	120	0.826
50	33.33	0.172	0.057	145.27	1.033
60	40.00	0.207	0.069	145.27	1.331
70	46.67	0.241	0.080	145.27	1.893
80.37	53.58	0.277	0.092	145.27	20.059

When the state of the soil transfers from elastic state to the yielding point as the lateral load increases, the lateral soil resistance does not change with increasing displacement and stay the same with the ultimate soil lateral resistance value with increasing displacement.

To be more specific about the analytical process of the Motta method for timber pole wall, the displacement value was resulted by h (dimensionless load), m (dimensionless moment) and Equation 19,20, and 23. Particularly, as the Table 5 illustrates, the Equation 19 is utilized for calculating the lateral displacement for the rows from 36 to 40 where the soil is in elastic state. Similarly, the Equation 20 is used the rows from 41 to 42 which is based on 50 kN to 60 kN where the soil yields from the upper part of the pile. Finally, the Equation 23 is utilized for calculating the lateral displacement in the row 43 and 44 where the soil yields from the bottom part of the pile. Moreover, the rows representing the lateral load from 80.5 kN to 145.2 7kN were turned out to be unrealistic value for the soil-pile system in real world referring to the Motta method (Motta, 2013). Concerning the soil lateral resistance value that is less than the ultimate soil lateral resistance value in the spreadsheet, the Equation 26 was utilized from row 36 to 40 until it reaches the ultimate soil lateral resistance which is resulted by the Georgiadis method. The five sets of spreadsheets for different pile spacing and different soil strength are attached in Appendix.

3.1.4 The P-y Curve For the Timber Pole Wall By Analytical Method (S/D=2, D=500 mm, And Strength=50 kPa)

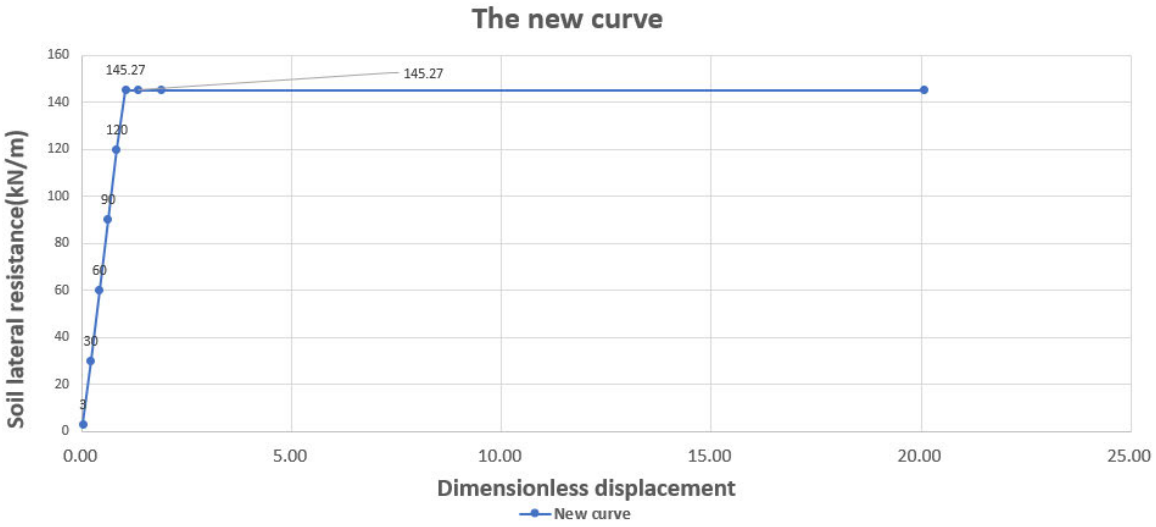

Figure 15: The newly plotted p-y curve (S=1m, D=0.5m, and strength=50kPa)

The p-y curve in Figure 15 is plotted from the data of spreadsheet in Table 5. As Figure 15 illustrates, the p-y curve shows the elastic-plastic behaviour where the soil lateral resistance sharply increases to the ultimate soil lateral resistance value and stays the same with increasing displacement when it reaches to the maximum soil lateral resistance. In this graph, the ultimate soil lateral resistance value is 145.27 kN/m. For the data on x-axis, the displacement of the p-y curve is expressed in dimensionless form.

3.1.5 The P-y curve For The Timber Pole Wall By Reese Method (S/D=2, D=500 mm, And Strength=50 kPa)

Table 6: The spreadsheet of the data from the Reese method

Reese method	
y_{so}	1.25
ε_{so}	0.01
Soil resistance(kN/m)	Displacement (cm)
1	3.26674E-08
10	0.0003
20	0.0052
30	0.0265
40	0.0836
50	0.2042
60	0.4234
70	0.7843
80	1.3381
90	2.1433
100	3.2667
110	4.7828
120	6.7739
130	9.3301
140	12.5495
157.3	20.0000

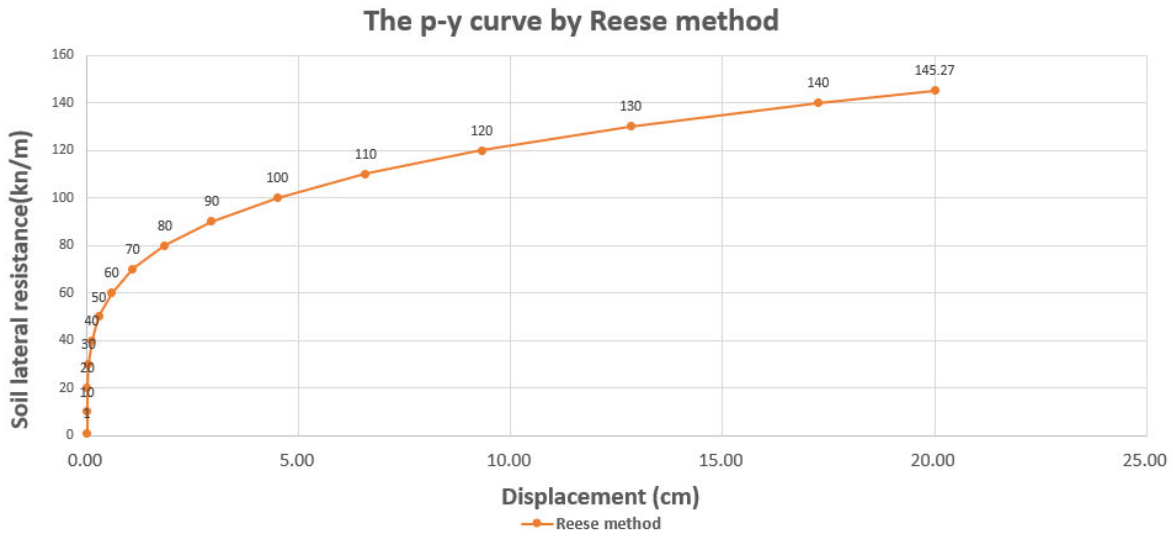

Figure 16: The p-y curve by Reese method

Using the Equation 1 and Equation 5, the p-y curve was plotted by Reese method which is classic analytical method for plotting the p-y curve. Unlike the analytical method, the displacement resulted from the Reese method has the dimension. The p-y curve reaches its ultimate soil lateral resistance which is 145.27 kN/m in the displacement of 20 cm.

3.1.6 Comparison Of the Newly Plotted P-y curve With the P-y curve By The Reese Method

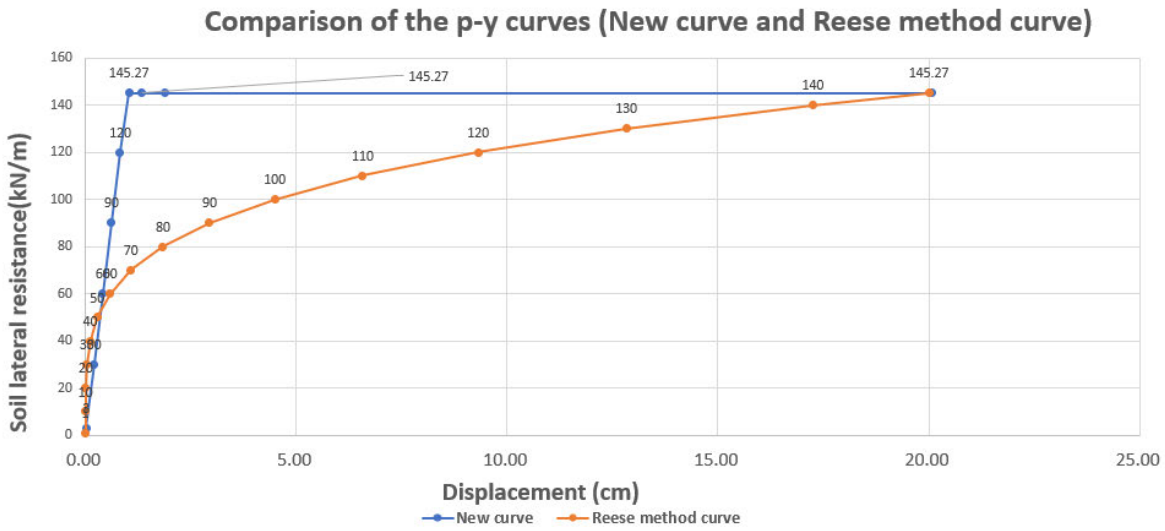

Figure 17: Newly plotted p-y curve and p-y curve by Reese method

Figure 17 shows the comparison of newly plotted p-y curve with Reese method curve. Specifically, the newly plotted p-y curve for timber pole walls shows a steep slope reaching the ultimate lateral resistance in smaller displacement whereas the Reese method curve shows smooth curve.

3.1.7 Comparison Of the Newly Plotted P-y Curve With The P-y Curves By The Reese method and Matlock method

Table 7: The spreadsheet of the data by Matlock method

Matlock method	
y_{50}	2.5
ε_{50}	0.02
Lateral load(kN/m)	Displacement(cm)
1	8.99898E-08
10	0.0009
20	0.0144
30	0.0729
40	0.2304
50	0.5624
60	1.1663
70	2.1607
80	3.6860
90	5.9042
100	8.9990
110	13.1754
120	18.6603
130	25.7020
140	34.5705
145.2	40.0000

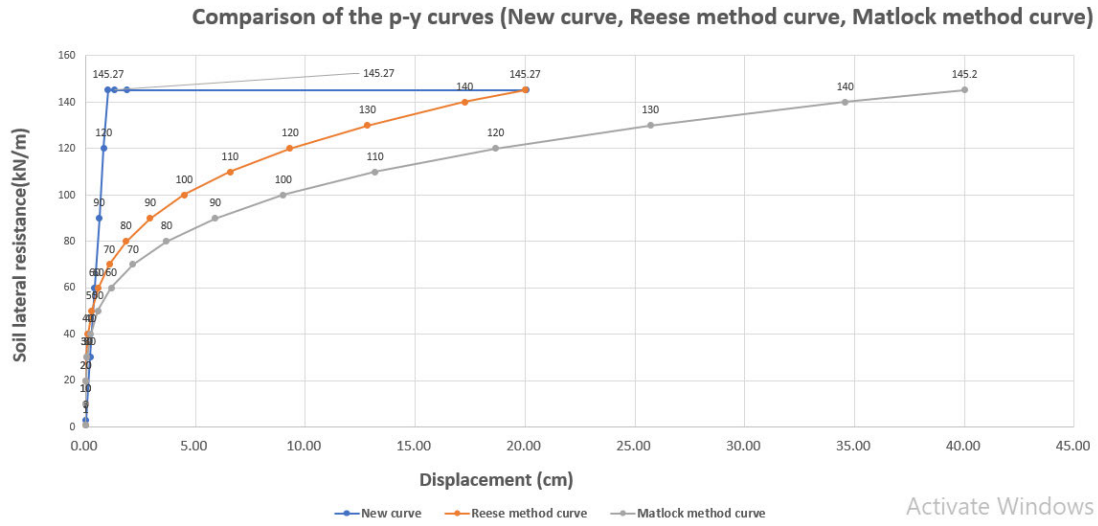

Figure 18: The newly plotted p-y curve, Reese method curve, and Matlock method curve

The newly plotted p-y curve was compared with the curve from Reese method and the curve from Matlock method. For the curve from Matlock method, the displacement showed bigger value compared to newly plotted p-y curve and Reese method which was 40cm. This is because the Matlock method's normal strain value is 0.02 which is suitable for soft clay environment

while the newly plotted p-y curve and Reese method curve were plotted based on medium stiff clay. Since this project is focused on medium stiff clay where the undrained shear strength is between 50 kPa and 200 kPa, the Reese method curve was mainly analysed and utilised for the project.

3.2 Numerical Analysis

When the digital computers were developed and commercialized throughout the world during mid-20th century, the increasing demand for sophistication of the mathematical models in science and engineering led to the creation of the various software that based on numerical solution. The most renowned numerical analysis technique for the software is the finite element method (Atkinson, 2017). This method is not only used in material engineering and mechanical engineering but also actively used in civil engineering discipline for various academical and industrial projects.

3.2.1 RSPile

The RSPile software was developed by Rocscience Inc in Canada. It can be used for the axial load capacity analysis of piles and analysis of piles under lateral loading is capable. Specifically, under the condition of various types of loading, RSPile can calculate the pile head displacement as well as the soil lateral resistance which are essential to plot the numerical p-y curves. This software is utilized for numerical analysis of this project.

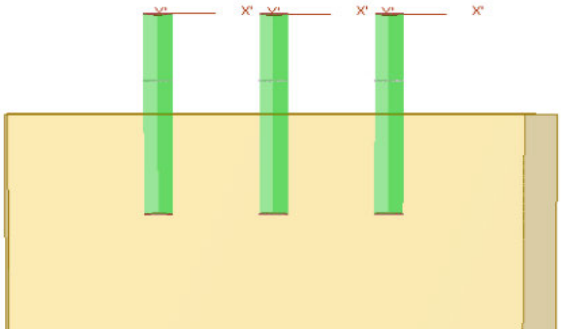

Figure 19: The front view of the RSPile model

Figure 19 represents the front view of the RSPile model where three piles are installed in the ground adapted from RSPile software. RSPile can customize the pile properties by specifying the shape of the cross-section of the pile and young's modulus of the pile material which is essential for this project since the detail of the timber pole strength value is inputted into the

project to simulate timber pole on the software. In addition to that, the normal strain, bulk unit weight and soil strength can be customized to simulate the same environment with analytical method. Not only individual pile can be analysed in the software but also group pile analysis is available. For the group pile analysis, the p-multiplier value is specified on the pile properties tab.

3.2.2 Basic Theory

Figure 20 represents the spring mass model to explain about the soil lateral resistance for p-y curve taken from Rocscience (2018).

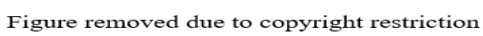

Figure 20: The spring mass model for p-y curve **(Rocscience, 2018)**

The first notion of the p-y curves was developed based on the concept of subgrade reaction modulus developed by Winkler (1867) and McClelland and Focht (1958). The concept of p-y curve is focused on the assumption where the pile is deemed as the beam on elastic foundation that is supported by the springs as the Figure 20 indicates (Bouafia, et al., 2018). In other words, researchers assumed that elastic pring of the ground is proportional to the load that applied to the pile and stiffness of the ground is assumed as the spring constant (Basu, et al., 2008). Specifically, the spring have relevance to the resistive properties of the soil element below the ground surface. (Basu, et al., 2008). Moreover, the spring constants are generally resulted from empirical equations (Basu, et al., 2008).

Additionally, Hetenyi (1946) assumed the pile-soil interaction as the beam on the springs and developed a differential equation (Levy, 2007).

$$E_p I_p \frac{d^4 u_x(z)}{dz^4} + K_r(z) u_x(z) = 0 \qquad \text{Equation 27}$$

Where E_p is the Young's modulus of the pile;

I_p signifies the second moment area of the pile

$K_r(z)$ represents the modulus of the subgrade reaction

$u_x(z)$ indicates the lateral displacement of the pile

(z) is the depth below the pile head

3.2.3 Software Modelling

3.2.3.1 Specification of Soil Properties and the Pile Properties

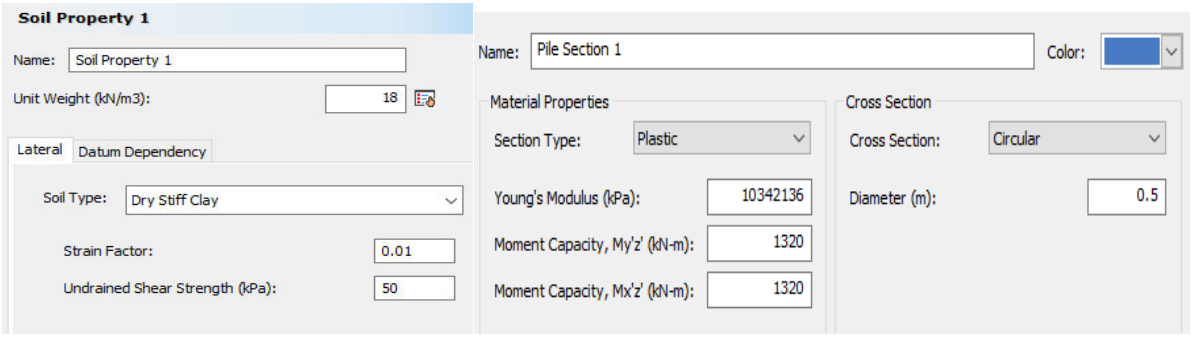

Figure 21: The soil property and pile properties

The bulk unit weight of the clay material is specified as 18 kN/m^3 and the values of the undrained shear strength for this project are from 50 kPa to 200 kPa. The Young's modulus of the timber pole is 12000000 kPa (Pender & Rodgers, 2017) and the diameter of the timber pole is 0.5 m. The moment capacity of the timber pole was calculated by the Young's modulus value and the Equation 28.

$$M = \frac{EI}{r} \qquad \text{Equation 28}$$

Where E is the Young's modulus of the timber pole, I is the geometric moment of intertia of the timber, and r is the radius of the timber pole. With regards to the symbol of I, this value was calculated by Equation 29 as the cross-section of the timber pole is circular.

$$I = \frac{\pi}{4} \times r^4 \qquad \text{Equation 29}$$

3.2.3.2 Specification of Pile Type and Loading

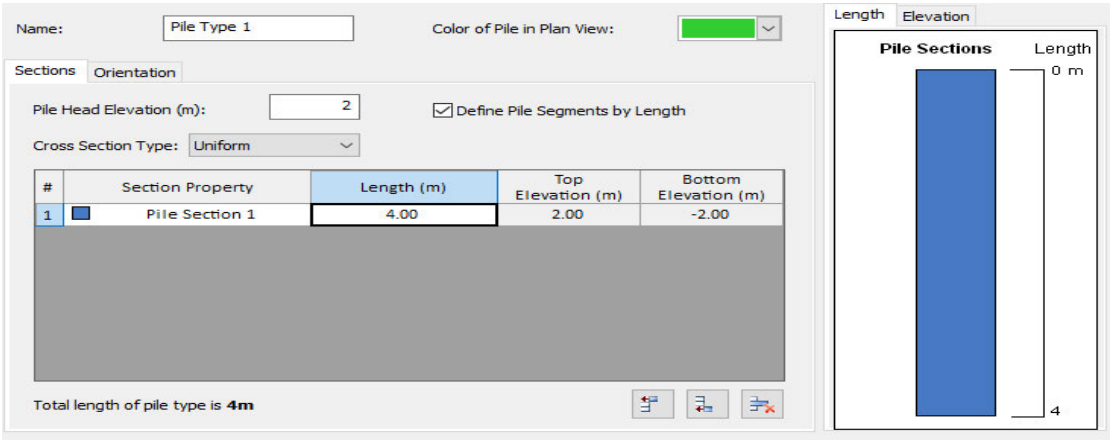

Figure 22: The pile length

Regarding the total length of the timber pole, it was 4 m. The pole height above the ground surface is 2 m which is same with the embedded length of the pole below the ground surface.

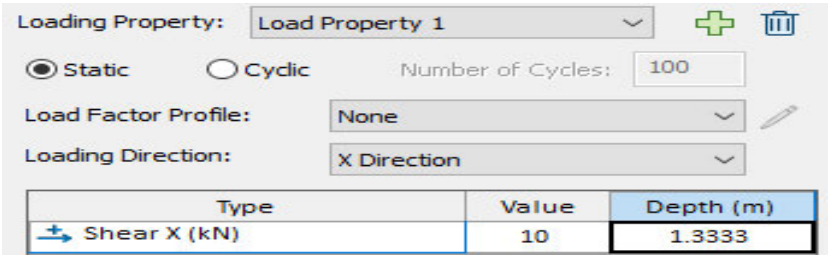

Figure 23: The load property

For the loading property, since earth lateral resultant force is applied to the pole, the load is determined as the static load. The lateral load is applied to the 1/3 of the wall height above the ground surface referring to the Rankine earth pressure method. The lateral load increases from 10 kN to the ultimate load when the soil lateral resistance reaches to the ultimate soil lateral resistance.

3.2.3.3 The Model of The Three Piles in RSPile

Figure 24: The model of the RSPile

As Figure 24 illustrates, the pink region of the model indicates the sand material which is backfill region above the excavated ground level. The thickness of the sand region is 2 m which accords to the height of the retaining wall above the excavated depth. To be more specific, the lateral pressure of the backfill region which accords to the pink coloured region in Figure 24 is applied to the pole as a form of resultant force in this project. Along with that, the yellow region represents the clay region below the excavated ground surface where the lateral soil resistance is analysed.

3.2.3.4 The Illustrative Profile of the Lateral Soil Resistance

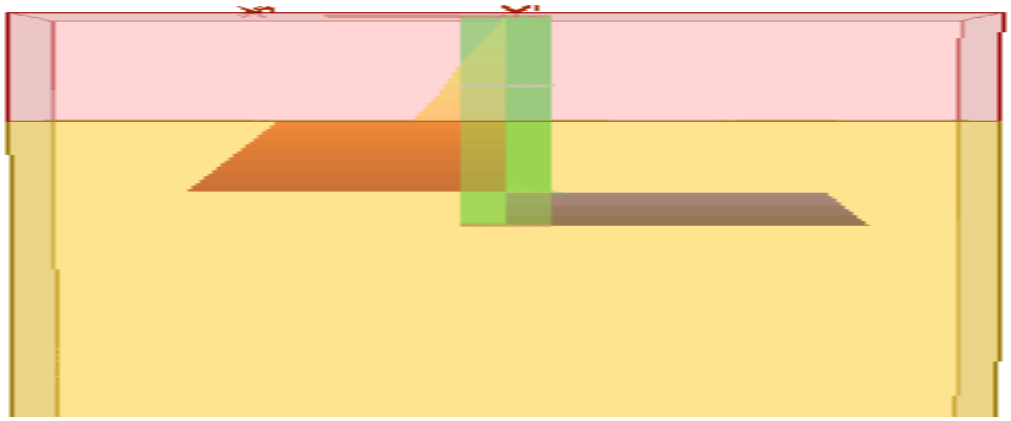

Figure 25: The soil reaction force profile from RSPile

Figure 25 is the illustrative soil reaction force profile when the pile is loaded from lateral force. The soil reaction force is referred as the soil lateral resistance for the analysis. The lateral load was applied to the grey line of the pile which is 1.3333 m below the pile head. The red region of the soil reaction profile represents the forward movement of the pile above the rotation point.

Moreover, the blue region indicates the backward movement of the pile below the rotation point.

3.2.3.5 The Illustrative Example of the P-Y Curve from Software Analysis (RSPile)

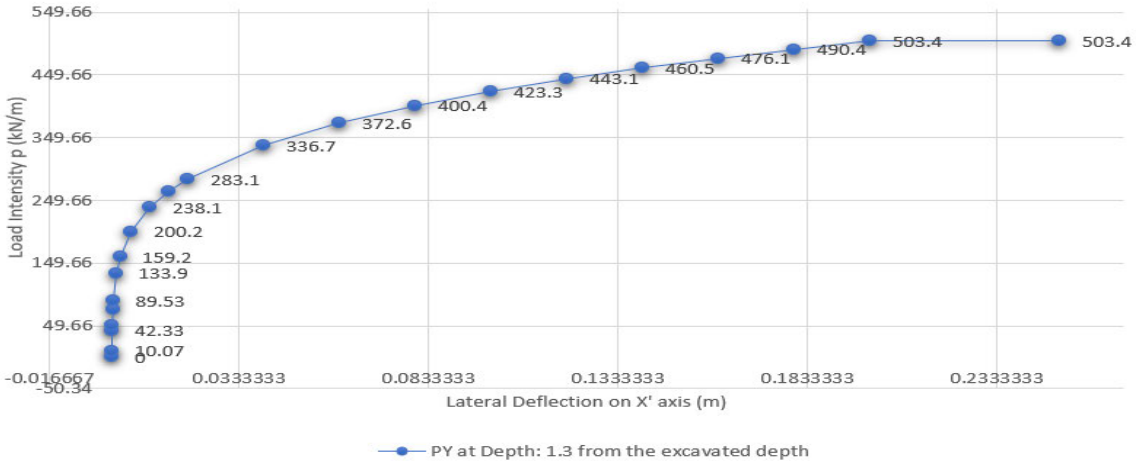

Figure 26: The p-y curve from RSPile

Figure 26 represents the illustrative p-y curve resulted at depth of 1.3 m below the excavated ground surface for the timber pole wall.

3.2.3.6 Comparison the Numerical Modelling with Classic Analytical Method

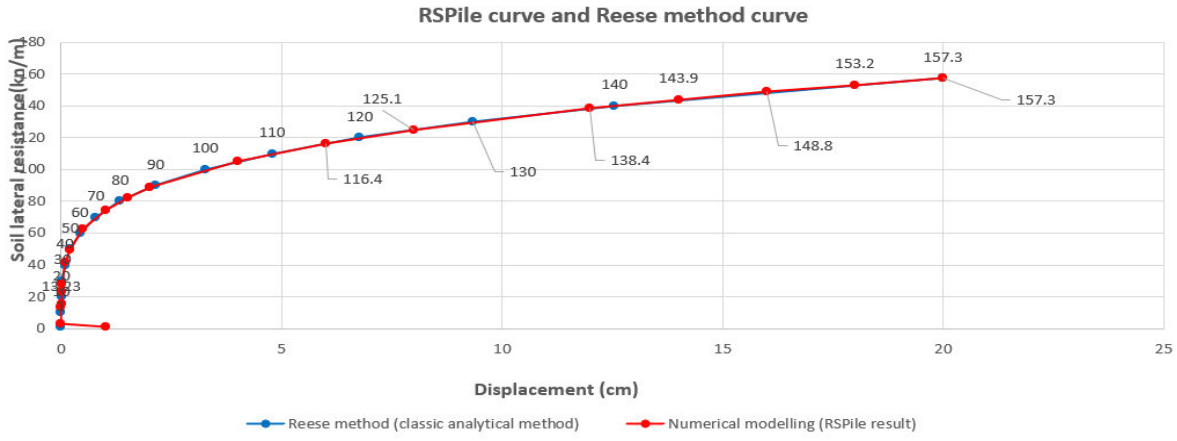

Figure 27: The p-y curves from numerical modelling and Reese method

To check the modelling accuracy of the software, which is RSPile, the result from RSPile was compared to the result from the Reese method on identical condition. Specifically, on the condition of the wall where the pole spacing is 1 m, pole diameter is 0.5 m and the soil strength is 50 kPa, the p-y curves from numerical modelling and classic analytical method which is Reese method are compared with each other in Figure 27. The result of the data from the Reese method was plotted in the blue coloured graph. Following this, the result of the data from numerical modelling was plotted in the red coloured graph in Figure 27. As Figure 27 illustrates, the trend of the p-y curve from numerical modelling is almost identical with the trend of the p-y curve from the classic analytical method, which is the Reese method. This might be due to the fact that the software RSPile is developed and programmed referring to various analytical methods such as Matlock method and Reese method. As a result, from the Figure 27, it can be concluded that the result of the RSPile software meet the required modelling accuracy.

4 RESULT AND DISCUSSION

4.1 P-y Curves For Different Soil Strength and Spacing

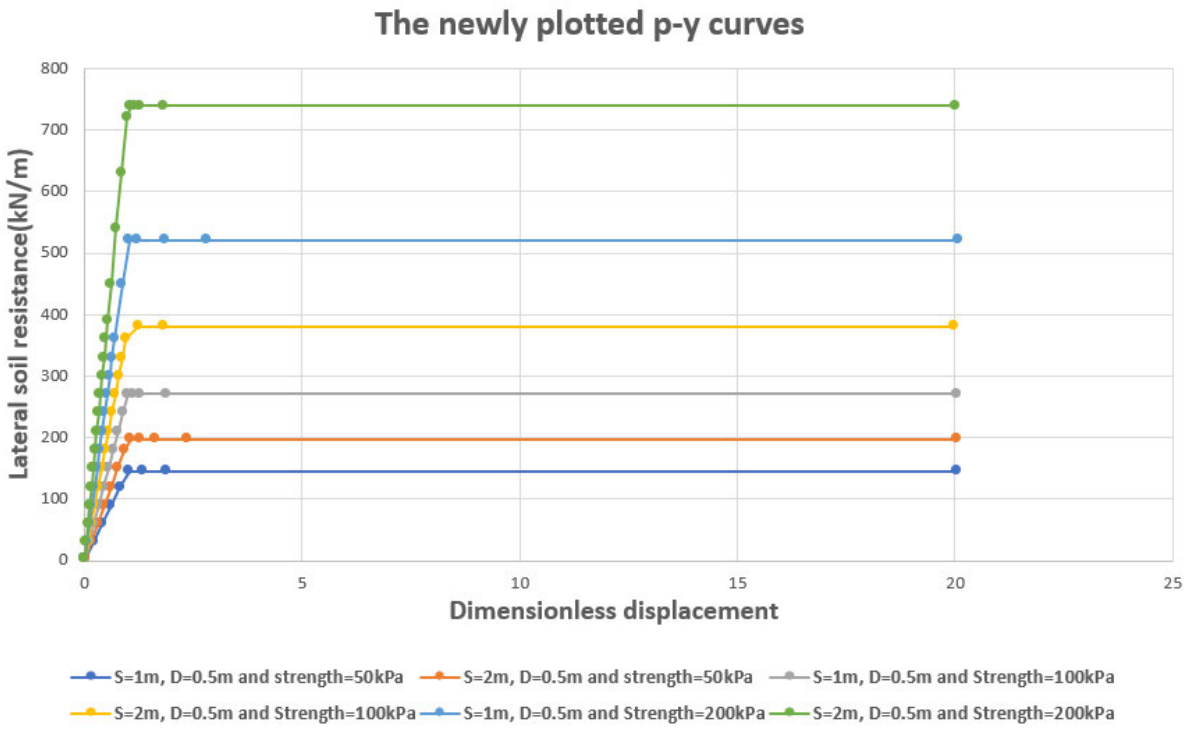

Figure 28: The newly plotted p-y curves (combining Georgiadis method and Motta method)

The six sets of p-y curves are resulted in in terms of the two different pile spacings (S/D=2 and 4) and the three different soil strengths (undrained shear strength=50,100, and 200 kPa) by analytical methods which is based on the Georgiadis method and the Motta method.

From the six p-y curves shown in Figure 28, the following conclusions can be drawn:

(1) All of the newly plotted p-y curves show elasto perflectly plastic curve. In other words, the p-y curves in Figure 28 shows linear increase up until it reaches the dimensionless displacement of 1. After it reaches the dimensionless displacement of 1, the trend of the whole p-y curves shows the tendency to maintain same lateral soil resistance with increasing displacement which shows ultimate soil resistance around the timber pole below the ground surface. Since the soil lateral resistance reaches its maximum value on small displacement, which is 1, the slope of all the p-y curves plotted by new method shows a fairly steep trend in early stage.

(2) When the the undrained shear strength of the clay gets larger, the lateral soil resistance shows the tendency that the value of it also gets larger. For instance, the ultimate lateral soil resistance is from 145.27 kN/m to 197.62 kN/m for clay strength of 50 kPa. However, the ultimate lateral soil resistance is from 521.135 kN/m to 739.034 kN/m when the clay strength is 200 kPa.

(3) The timber pole wall that has narrow pole spacing results in the smaller soil lateral resistance compared to the timber pole wall that has wide pole spacing. In detail, when the timber pole wall is installed on the condition that has the 1 m pole spacing, 0.5 m diameter and 50 kPa soil strength, the lateral soil resistance of it was lower than that of the wall that is installed on the condition that has 2 m pole spacing, 0.5 m diameter and 50kPa soil strength because of pile reduction effect.

(4) Noticeably, the difference of the two ultimate soil lateral resistances of the wall that has clay strength of 200kPa which is located on the top of the Figure 28 seems much larger than the difference of the two ultimate soil lateral resistances of the wall that has clay strength of 50 kPa which is located on the bottom of the Figure 28.

4.2 The Result of the RSPile Analysis (Numerical Method)

The software analysis is performed in terms of two different pile spacings (S/D=2 and 4) and the three different soil strengths (undrained shear strength=50,100, and 200 kPa). The software analysis's wall specification and soil parameters are unified with the analytical method for comparison process. Regarding the p-y curves from the software, the p-y curves at depth of 1.3 m below the ground surface were mainly analysed for comparison with newly plotted p-y curves.

4.2.1 The P-y Curves plotted from the RSPile Software

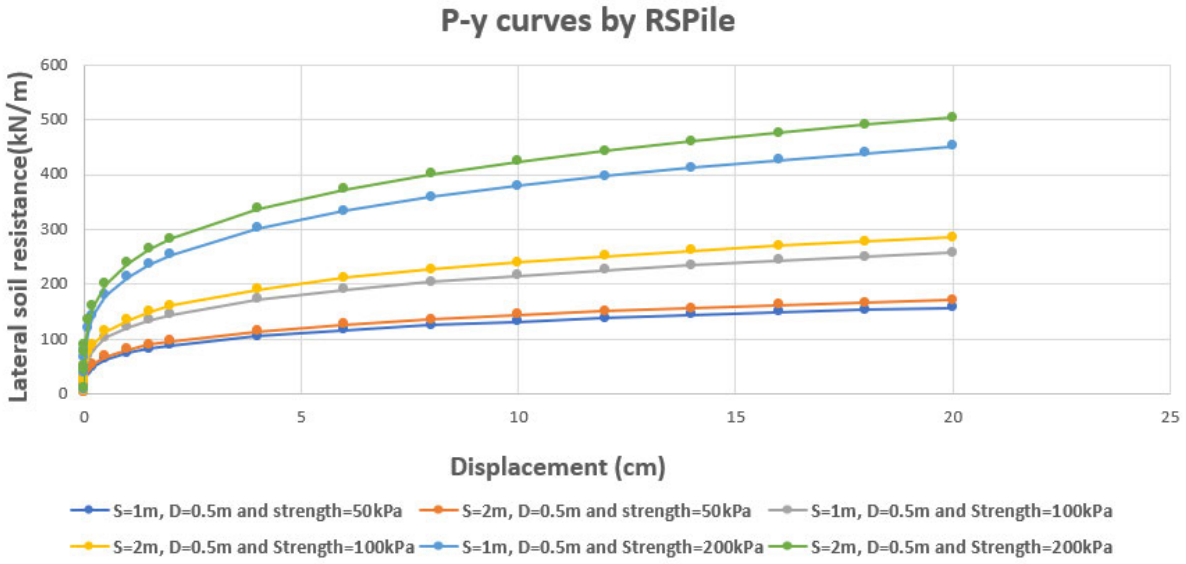

Figure 29: The p-y curves from RSPile

The six sets of p-y curves plotted from the data resulted from RSPile software reaches its ultimate soil lateral resistance on the displacement of 20 cm. To unify the test conditions with analytical method, the soil strength values of 50 kPa,100 kPa, and 200 kPa were selected. Additionally, the two different pile spacings were S/D of 2 and 4.

From the six p-y curves shown in Figure 29, the following conclusions can be drawn:

(1) When the undrained shear strength of the clay increases, the lateral soil resistance also increases. For instance, the ultimate lateral soil resistance is from 157.3 kN/m to 170.9 kN/m for clay strength of 50 kPa. However, the ultimate lateral soil resistance is from 451.1 kN/m to 503.4 kN/m when the clay strength is 200 kPa.

(2) The timber pole wall that has narrow pole spacing results in the smaller soil lateral resistance compared to the timber pole wall that has wide pole spacing. To be more specific, when the timber pole wall is constructed on the condition that has the 1m pole spacing, 0.5 m diameter and 50kPa soil strength, the lateral soil resistance of it was lower than that of the wall of 2 m pole spacing, 0.5 m diameter and 50 kPa soil strength.

(3) The gap of the lateral soil resistance between the two curves due to pile spacing effect on same soil strength increases as the undrained shear strength of the clay increases. Specifically, when the timber pole is installed on the clay with 50 kPa undrained shear strength, the gap of the ultimate lateral soil resistance due to pile spacing effect on 50 kPa clay is turned out to be 13.7 kN/m from 157.3 kN/m to 170.9 kN/m. The gap of the ultimate lateral soil resistance due to pile spacing effect on 200 kPa clay is turned out to be 52.3 kN/m from 451.1 kN/m to 503.5 kN/m.

4.3 Comparison of P-y Curves

In this section, the p-y curves plotted by both methods which are analytical method and RSPile software are compared with each other in terms of three different clay strength.

4.3.1 The Clay Strength of 50 kPa

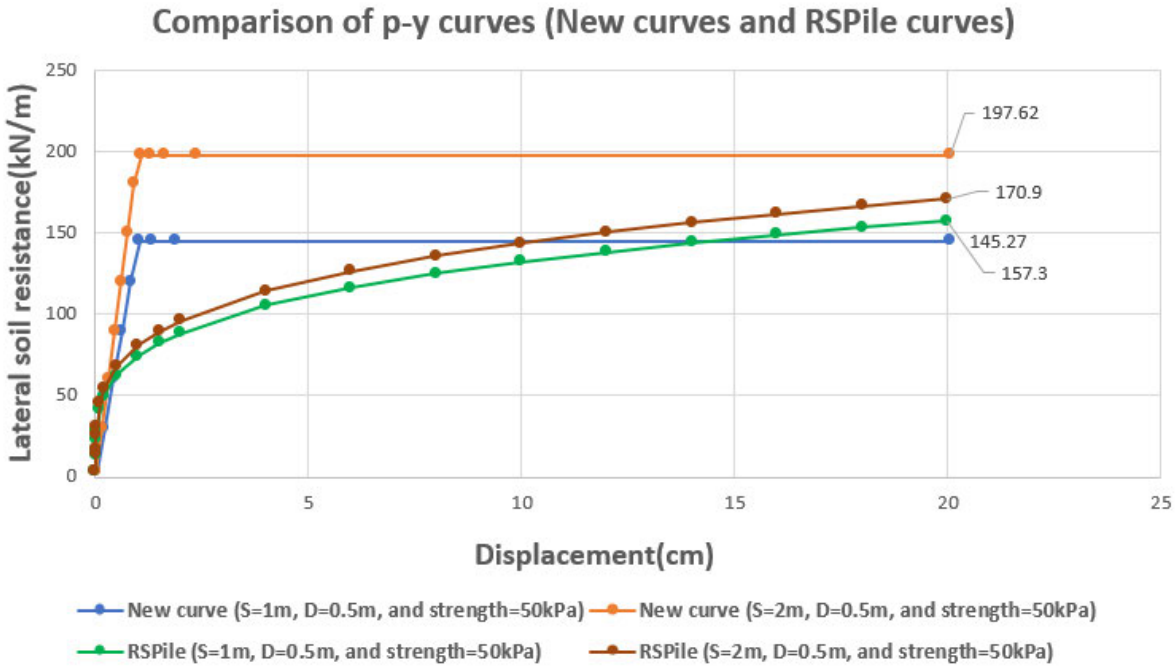

Figure 30: Comparison of the p-y curves (Strength=50kPa)

Figure 30 illustrates the p-y curves plotted by analytical method and RSPile software analysis. All of the p-y curves in Figure 30 were plotted on the basis of the 50 kPa undrained shear strength of the clay.

From Figure 30, there are some points can be concluded:

(1) As Table 8 shows, the difference of the ultimate soil lateral resistance value between new curve and curve from RSPile is 8.3% for the wall that has spacing of 1m, diameter of 0.5 m and clay strength 50 kPa. Also, the difference of the ultimate soil lateral resistance value increases to 15.6% when the pile spacing increases to 2 m.

Table 8: Difference of ultimate soil lateral resistance between new curve and RSPile (50 kPa)

Pole Specifications	Ultimate Soil Lateral Resistance (kN/m)		Difference (%)
	New Curve	RSPile	
S=1 m, D=0.5 m, and strength=50 kPa	145.27	157.3	8.3
S=2 m, D=0.5 m, and strength=50 kPa	197.62	170.9	15.6

(2) Especially in the small displacement value, the new p-y curves show much larger soil resistance than that of the p-y curves resulted from the RSPile. It might be due to the fact that RSPile is basically programmed referring to the classic analytical methods such as Matlock method and Reese method where polynominal equations are present in those two methods. The classic methods do not classify the soil state depending on the extent of the lateral load and express the soil lateral resistance and displacement value in just only one equation as it can be seen in Equation 5. So, this might be the biggest reason that raise the discrepancy of the results between new p-y curve and p-y curve from RSPile.

4.3.2 The Clay Strength of 100kPa

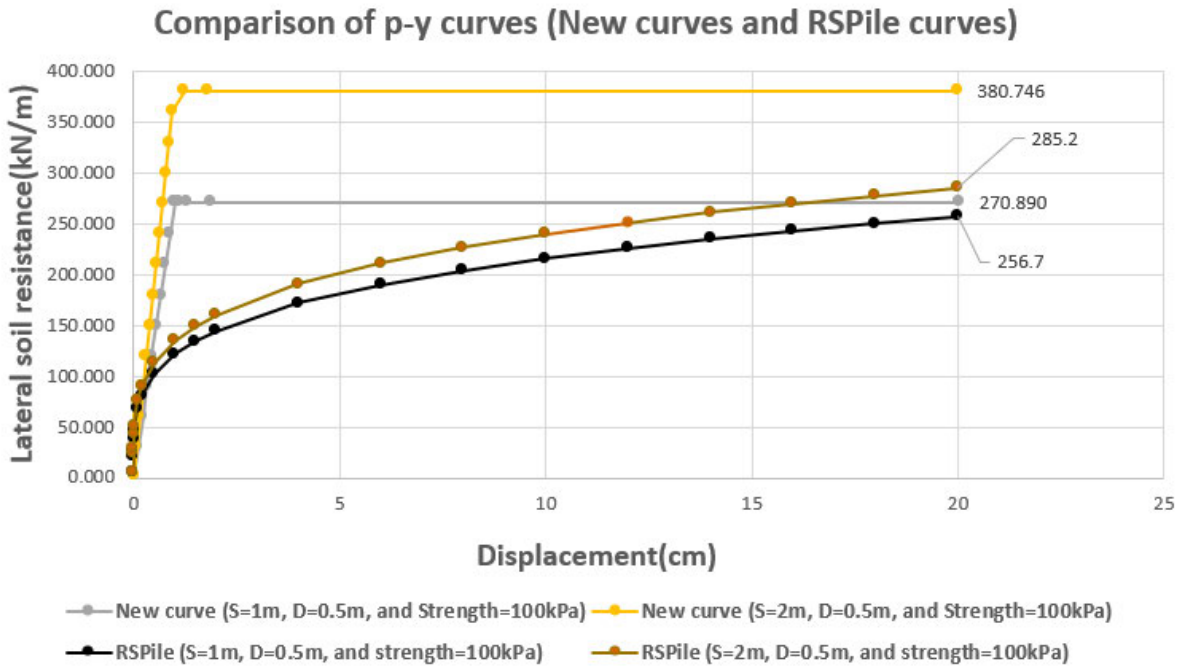

Figure 31: Comparison of the p-y curves (Strength=100kPa)

Figure 31 represents the p-y curves plotted by analytical method and RSPile software analysis which are mainly based on the 100kPa undrained shear strength of the clay.

From the graphs in Figure 31, there are some points can be concluded:

(1) As Table 9 shows, the difference of the ultimate soil lateral resistance value between new curve and the curve from RSPile is 5.5% for the wall that has spacing of 1 m, diameter of 0.5 m and clay strength 100 kPa. The difference of the ultimate soil lateral resistance value increases to 33% when the pile spacing of the wall increases to S=2 m from S=1 m.

Table 9: Difference of the ultimate soil lateral resistance value between new curve and RSPile curve (100kPa)

Pole Specifications	Ultimate Soil Lateral Resistance (kN/m)		Difference (%)
	New Curve	RSPile	
S=1 m, D=0.5 m, and strength=100 kPa	270.89	256.7	5.5
S=2 m, D=0.5 m, and strength=100 kPa	380.746	285.2	33

(2) Compared to the p-y curves which are based on the 50kPa clay strength, the pile spacing effect (pile group reduction effect) of all p-y curves based on 100kPa clay strength is more prominent on both analytical method and RSPile software analysis. Specifically, the gap of the ultimate soil lateral resistance due to pile spacing effect is ranging from 8.65% to 36% for 50kPa clay strength. However, for the p-y curves with 100kPa clay strength, the gap of the ultimate soil lateral resistance due to pile spacing effect increases to from 11.1% to 40.6%. Thus, it can be concluded that the pile spacing effect is also getting more prominent as the undrained shear strength of the clay increases on both the new curve and the curve from RSPile analysis.

4.3.3 The Clay Strength of 200 Kpa

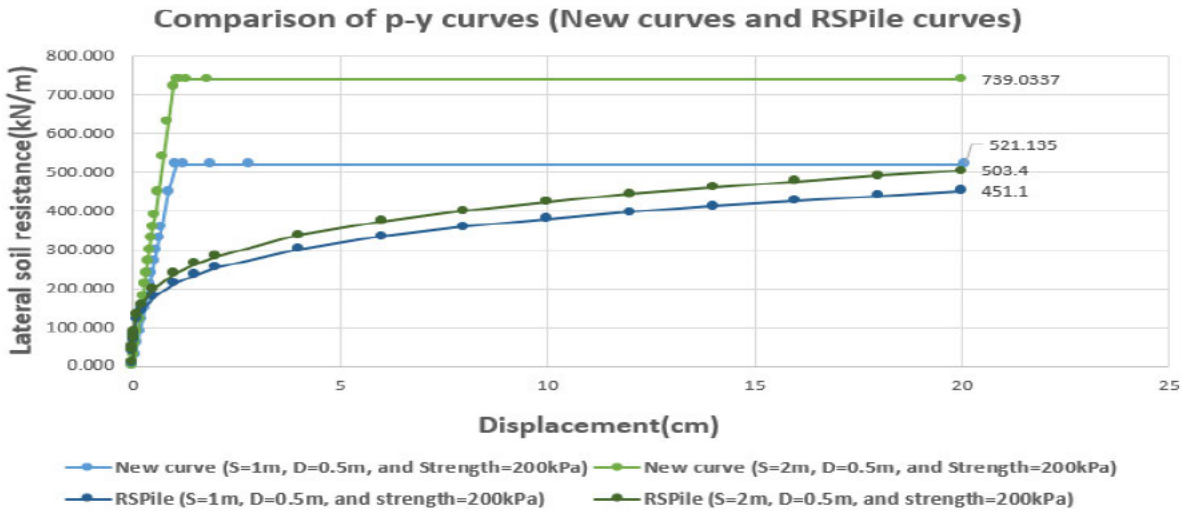

Figure 32: Comparison of the p-y curves (strength=200kPa)

Figure 32 represents the p-y curves plotted by analytical method and RSPile software analysis which are mainly based on the 200kPa undrained shear strength of the clay.

From the p-y curves in the Figure 32, there are some points can be concluded:

(1) The pile spacing effect (pile group reduction effect) of the p-y curve is the most prominent in the 200kPa clay strength compared to the 50 kPa clay strength and the 100 kPa clay strength. Specifically, the difference of the ultimate soil lateral resistance due to pile spacing effect (pile group reduction effect) in new method is 41% from 521.135 kN/m to 739.034 kN/m. The difference of the ultimate soil lateral resistance due to pile spacing effect in Software analysis is 11.6%. Table 10 visualizes the pile spacing effect on each clay strength.

Table 10: The different pile spacing effect in different strength of clay.

Undrained shear strength of clay	Pile spacing effect in new curve (Georgiadis and Motta method)	Pile spacing effect in RSPile curve
50kPa	36%	8.65%
100kPa	40.6%	11.1%
200kPa	41%	11.6%

As Table 10 illustrates, the pile spacing effect in both methods has a tendency that the effect is getting more prominent as the undrained shear strength of clay increases. This phenomenon is related to the characteristic of pile group reduction effect equation devised by Georgiadis et al (2013) using analytical upper bound calculations. Using the Equation 7,8,9 and 10, the group pile reduction factor was resulted in the middle of the analytical method process.

Table 11: The group pile reduction factor

Pole Specifications	**Group pile reduction factor (f_{mug})**	**Absolute value of the difference**
Spacing=1m, Diameter=0.5m, and strength=50kPa	0.912	0.079

Spacing=2m, Diameter=0.5m, and strength=50kPa	0.991	
Spacing=1m, Diameter=0.5m, and strength=100kPa	0.9	0.1
Spacing=2m, Diameter=0.5m, and strength=100kPa	1	
Spacing=1m, Diameter=0.5m, and strength=200kPa	0.896	0.104
Spacing=2m, Diameter=0.5m, and strength=200kPa	1	

As Table 11 illustrates, since the absolute value of the pile group reduction factor difference increases, the soil lateral resistance which is affected by this pile group reduction factor also end up having the value where their values between different pile spacings result in greater difference as the undrained shear strength of the clay increases. This phenomenon is also present in RSPile analysis as Figures 30,31,32 indicate.

(2) From Tables 8, 9, and 12, it is evident that the discrepancy in ultimate soil lateral resistance between the new curves and those from RSPile analysis increases with increasing undrained shear strength. This difference is particularly significant in very stiff clay environments, indicating that the p-y curves do not align well with the software curves in these conditions. Additionally, the discrepancy in ultimate soil lateral resistance between the new curve and the RSPile curve is larger for larger pile spacings.

Table 12: Difference of ultimate soil lateral resistance between new curve and RSPile curve (200kPa)

Pole Specifications	Ultimate Soil Lateral Resistance (kN/m)		Difference (%)
	New Curve	RSPile	
S=1m, D=0.5m, and strength=200kPa	521.135	451.1	15.5
S=2 m, D=0.5 m, and strength=100 kPa	739.034	503.4	46

5 CONCLUSION

- From this project, it can be concluded that the newly plotted p-y curves require further research as it turns out that there is significant difference in ultimate soil lateral resistance value between new p-y curves and software curves especially in stiff clay and very stiff clay.
- Especially on the small displacement, the soil lateral resistance of the newly plotted p-y curve shows larger value than the p-y curve of software analysis.
- The first reason of the difference of the soil latereal resistance is that software which was developed based on classic methods might have resulted in conservative value for the soil lateral resistance in small displacement as the classic methods do not classify the soil state in terms of the intensity of the applied lateral load to the pile.
- The other factor that might have caused the difference of the result between the new curves and curves from RSPile analysis is that the software modelling could not fully simulate the exact environment of the timber pole walls. Specifically, even though the sand layer which indicates the backfill region was on top of the clay layer in software modelling, the excavation work was not possible for the sand layer in RSPile software.
- The newly plotted p-y curves show pile reduction effect on three different strength cases which are crucial for timber pole wall design as the timber pole wall consists of a group of timber poles.
- From the newly plotted p-y curves, the pile group reduction effect is not same on all three strength cases. In fact, the pile group reduction effect is getting more prominent in both newly plotted p-y curves and RSPile analysis as the undrained shear strength increases.
- The surcharge load of the backfill region for the timber pole wall was small for this project which was $\frac{q}{q_u} = \frac{2*16}{5.2*50} = 0.123$. As the timber pole wall has the height from 1.5 m to 3.5 m, the surcharge load could not exceed the value of $\frac{q}{q_u} = 0.5$ as the timber pole wall is only for low to moderate height excavation work. As a result, the pile group reduction effect of the timber poles gave a bigger impact to the wall than surcharge load effect as the timber pole wall has low height compared to the soldier pile walls.

6 FEEDBACK FOR FUTURE WORK BASED ON THE PROJECT OUTCOME

The software that was utilized for numerical modelling process for this project was RSPile which was developed by Rocscience Inc in Canada. The excavation work was not available for the numerical modelling on this software which was crucial for the project. Hence, the data from the RSPile software might not have been perfectly suitable for comparison process with the newly plotted p-y curves. For the future work, the Plaxis 3D and PYWALL software can be utilized where excavation work is available on the software as these two softwares will simulate the exact environment of the timber pole walls.

7 FUTURE WORK AND RECOMMENDATION

This project was mainly focused on the forward movement of the pile below the ground surface as this movement takes part of 65 % of the whole embedment length. From this point, future work might focus on the plotting process of the p-y curves for the backward movement of the timber poles below the rotation point. Hence, a recommend future work can focus on the different height and different types of the retaining wall such as tied-back timber pole walls since this project is for timber pole walls without any further measure such as struts. It can be anticipated that the surcharge load effect will have a significant impact on lateral soil resistance for the wall that has a height of over 5 m. In addition, the limitation of the newly plotted p-y curves is that the lateral displacement of the p-y curves is in dimensionless form which means the new p-y curves might not be perfectly suitable for real-world design process at the moment. Thus, the future work can focus on the plotting process of the p-y curves that has dimension for the lateral displacement.

BIBLIOGRAPHY

Abdul Kaream, K., Fattah, M. & Khaled, Z., 2020. Assessment of Changes in Shear Strength Parameters for Soils below Circular Machine. *International Journal of Engineering,* 33(8), pp. 1491-1498.

Atkinson, K. E., 2017. *Numerical analysis,* s.l.: Encyclopedia Britannica.

Ayadat, T., 2021. Determination of the undrained shear strength of sensitive clay using some laboratory soil data. *Studies in Engineering and Technology,* 8(1), pp. 14-27.

Basu, D., Salgado, R. & Prezzi, M., 2008. *Analysis of Laterally Loaded Piles in Multilayered Soil Deposits,* West Lafayette: Purdue University.

Bergardo, D. & Kamon, M., 1991. *Ground Improvement Techniques.* Bangkok, 91h Asian RegionalConf.Soil Mech.Found.Eng'g.

Bouafia, A., Haouari, H., Lachenani, A. & Tachet, D., 2018. P-y curves for single piles under lateral loads-finite elements modelling. *ASEC conference in Jordan,* pp. 1-10.

Brafford, G. et al., 2002. *Timber pile design & construction manual,* Starkville: Southern Pressure Treaters' Association.

Chen, X. & Broecke, J. v. d., 2021. Experimental study on the adhesion factor of clay. *Terra et Aqua,* Volume 163, pp. 6-17.

Chong, E. E.-M. & Ong, D. E.-L., 2020. Data-driven field observational method of a contiguous bored pile wall system affected by accidental groundwater drawdown. *Geosciences 2020,* 10(268), pp. 1-21.

Dhir, R., Brito, J. d., Mangabhai, R. & Lye, C. Q., 2017. *Sustainable Construction Materials: Copper Slag.* 2nd ed. Duxford: Woodhead Publishing.

Diwalkar, A., 2020. Analysis and Design of Retaining Wall: A Review. *2ND International Conference on Communication & Information Processing,* pp. 1-4.

Ebrahimian, B. & Nazari, A., 2014. Predicting ε50 for Lateral Behavior of Piles in Marine Clay Using an Evolutionary Based Approach. *Internation Journal of Maritime Techonology,* Volume 2, pp. 15-28.

Fayyazi, M. S., Taiebat, M. & Finn, L., 2014. Group reduction factors for analysis of laterally loaded pile. *Canadian Geotechnical Journal,* Volume 51, pp. 758-769.

Fayyazi, M. S., Taiebat, M., Finn, L. & Ventura, C., 2012. *Evaluation of Group Factor Method for Analysis of Pile Groups.* Lisbon, Fifteenth World Conference on Earthquake Engineering.

Georgiadis, K., 2018. Lateral soil resistance on soldier piles or king posts in clay. *Géotechnique,* 68(12), pp. 1071-1084.

Georgiadis, K., Lyamin, A. V. & Sloan, S. W., 2013. Undrained limiting lateral soil pressure on a row of piles. *Computers and Geotechnics,* Volume 54, pp. 175-184.

Georgiadis, M. & Anagnostopoulo, C., 1999. Displacement of structures adjacent to cantilever sheet pile walls. *Soils and foundations,* 39(2), pp. 99-104.

Higgins, W., Vasquez, C., Basu, D. & Griffiths, D. V., 2013. Elastic solutions for laterally loaded piles. *Journal of geotechnical and geoenvironmental engineering,* 139(7), pp. 1096-1103.

Huang, Z. et al., 2023. Study on vertical load distribution of pile group-liquefied soil system under horizontal seismic environment. *Sustainability 2023,* 15(9549), pp. 1-21.

Ishenhower, W. M. & Wang, S. T., 2016. *Technical user's manual for Lpile 2016,* Texas: Ensoft, Inc..

Jaksa, M. B. & Kaggwa, W., 1992. *Normalised Shear Strength and Compressibility Charactersitcs of Adelaide Expansive Clay.* Adelaide, The University of Adelaide.

Jaska, M., 1992. Degree of saturation of the Keswick Clay within the Adelaide city area above the general groundwater. *International Society for Soil Mechanics and Geotechnical Engineering,* pp. 336-341.

Kong, D., Liu, Y., Deng, M. & Zhao, X., 2020. Analysis of influencing factors of lateral soil resistance distribution characteristics around monopile foundation for offshore wind power. *Applied Ocean Research,* Volume 97, pp. 1-10.

Lehane, B., Wang, H. & Bransby, F., 2022. Field and numerical study of the lateral response of rigid piles in sand. *Acta Geotechnica,* Volume 17, pp. 5573-5584.

Levy, N. H., 2007. *Modeeling multi-directional behaviour of piles using energy principles,* Crawley: University of Western Australia.

Medjnoun, A. & Bahar, R., 2016. Shrinking–swelling of clay under the effect of hydric cycles. *Springer,* 1(46), pp. 1-8.

Merzdorf, J., 2020. *Climate Change Could Trigger More Landslides in High Mountain Asia,* Greenbelt: NASA's Goddard Space Flight Center.

Mohammed, G. A. et al., 2002. *P-y curves for laterally loaded drilled shafts embedded in weathered rock,* Raleigh: North Carolina State University.

Motta, E., 2013. Lateral deflection of horizontally loaded rigid piles in elastoplastic medium. *Journal of Geotechnical and Geoenvironmental Engineering,* 139(3), pp. 501-506.

Patil, S. S. & Amir, B., 2015. Analysis and design of reinforced concrete stepped cantilever retaining wall. *International Journal of Research in Engineering and Technology,* Volume 4, pp. 46-67.

Pender, M. & Rodgers, P., 2017. *Numerical modelling of lateral load-deformation curves for timber poles.* Auckland, University of Auckland.

Perko, H., 2008. Lateral earth pressure on lagging in soldier pile wall systems. *The Journal of the Deep Foundations Institute,* 2(1), pp. 52-60.

Reese, L. C. & Van Impe, W. F., 2009. *Single piles and pile groups under lateral loading.* 2nd

ed. s.l.:CRC Press.

Rocscience, 2018. *Laterally loaded piles theory manual,* Toronoto: Roscience Inc.

Rollins, K. M. et al., 2006. Pile spacing effects on lateral pile group behavior. *Journal of Geotechnical and Geoenvironmental Engineering,* 132(10), p. 28.

Steven, K. L., 1988. *Development of p-y curves for analysis of laterally loaded piles in western Washington,* Washington: Washington State Transportation Center.

Suryasentana, S. K. & Lehane, B. M., 2016. Updated CPT-based p-y formulation for laterally loaded piles in cohesionless soil under static loading. *Geotechnique,* 66(6), pp. 445-453.

Terceros, M., Thieken, K. & Achmus, M., 2017. Evaluation of p-y approaches for piles in soft clay. *Offshore Site Investigation Geotechnics 8th International Conference Proceeding,* 1(8), pp. 724-731.

Timber Queensland, 2014. *Timber Garden Walls,* Queensland: Timber Queensland Limited.

Versace Timbers, 2023. *Benefits of Building a Wood Retaining Wall.* [Online] Available at: https://www.versacetimbers.com.au/benefits-of-building-a-wood-retaining-wall/ [Accessed 1 8 2023].

Wallender, L., Tynan, C. & Allen, S., 2023. *How Much Does Installing A Retaining Wall Cost?.* [Online]
[Accessed 1 8 2023].

Wang, G. & Sitar, N., 2006. *Nonlinear Analysis of a Soil-Drilled Pier System under Static and Dynamic Axial Loading,* s.l.: University of California, Berkeley.

Wang, H. et al., 2022. A simple rotational spring model for laterally loaded rigid piles in sand. *Marin Structures,* Volume 84.

Wang, Y. C. & Briaud, J. L., 2018. *Synthesis of load-deflection characteristics of laterally loaded large diamter drilled shafts: technical report,* Texas: Texas A&M Transportation Institute.

Wood, J., 2021. *Cantilever pole retaining walls,* s.l.: NZ Geotechnical Society.

Wood, J., 2021. *Cantilever pole retaining walls.* [Online].

Wood, J., 2021. Cantilever Pole Retaining Walls. *NZ GEOMECHANICS NEWS,* Issue 101.

Yalcin, A., 2007. The effects of clay on landslides: A case study. *Applied Clay Science,* 38(1-2), pp. 77-85.

APPENDIX A: RESULTS DATA

Strength=50kPa			
Pile spacing =1m, Pile diameter=0.5m		Pile spacing=2m, pile diameter=0.5m	
Displacement(cm)	Soil lateral resistance(kN/m)	Displacement(cm)	Soil lateral resistance(kN/m)
0.0002	3.146	0.0002	3.419
0.001	13.23	0.001	14.37
0.002	15.73	0.002	17.09
0.01	23.52	0.01	25.56
0.02	27.97	0.02	30.4
0.1	41.83	0.1	45.45
0.2	49.74	0.2	54.05
0.5	62.55	0.5	67.97
1	74.38	1	80.83
1.5	82.32	1.5	89.45
2	88.46	2	96.12
4	105.2	4	114.3
6	116.4	6	126.5
8	125.1	8	135.9
10	132.3	10	143.7
12	138.4	12	150.4
14	143.9	14	156.3
16	148.8	16	161.7
18	153.2	18	166.5
20	157.3	20	170.9
25	157.3	25	170.9

Figure 33: The software result from RSPile (strength=50kpa)

Strength=100kPa			
Pile spacing =1m, Pile diameter=0.5m		Pile spacing=2m, pile diameter=0.5m	
Displacement(cm)	Soil lateral resistance(kN/m)	Displacement(cm)	Soil lateral resistance(kN/m)
0.0002	5.134	0.0002	5.704
0.001	21.59	0.001	23.98
0.002	25.67	0.002	28.52
0.01	38.39	0.01	42.65
0.02	45.65	0.02	50.72
0.1	68.26	0.1	75.84
0.2	81.18	0.2	90.19
0.5	102.1	0.5	113.4
1	121.4	1	134.9
1.5	134.3	1.5	149.3
2	144.4	2	160.4
4	171.7	4	190.7
6	190	6	211.1
8	204.1	8	226.8
10	215.9	10	239.8
12	225.9	12	251
14	234.8	14	260.9
16	242.8	16	269.7
18	250	18	277.8
20	256.7	20	285.2
25	256.7	25	285.2

Figure 34: The software result from RSPile (strength=100kPa)

Strength=200kPa			
Pile spacing =1m, Pile diameter=0.5m		Pile spacing=2m, pile diameter=0.5m	
Displacement(cm)	Soil lateral resistance(kN/m)	Displacement(cm)	Soil lateral resistance(kN/m)
0.0002	9.022	0.0002	10.07
0.001	37.93	0.001	42.33
0.002	45.11	0.002	50.34
0.01	67.45	0.01	75.28
0.02	80.22	0.02	89.53
0.1	120	0.1	133.9
0.2	142.6	0.2	159.2
0.5	179.4	0.5	200.2
1	213.3	1	238.1
1.5	236.1	1.5	263.5
2	253.7	2	283.1
4	301.7	4	336.7
6	333.8	6	372.6
8	358.7	8	400.4
10	379.3	10	423.3
12	397	12	443.1
14	412.6	14	460.5
16	426.6	16	476.1
18	439.4	18	490.4
20	451.1	20	503.4
25	451.1	25	503.4

Figure 35: The software result from RSPile (strength=200kPa)

Table 13: The spreadsheet for S=2m, D=0.5m, and strength=50kPa

Lateral load(kN)	Moment(kN*M)	h(dimensionless load	m(dimensionless moment)	Soil resistance (kN/m)	Normalised displacement	
		H/Plim/L	M/Plim/L			
1.00	0.67	0.00	0.00	3.00	0.02	CASE 1(Elastic)
10.00	6.67	0.03	0.01	30.00	0.15	CASE 1(Elastic)
20.00	13.33	0.05	0.02	60.00	0.30	CASE 1(Elastic)
30.00	20.00	0.08	0.03	90.00	0.46	CASE 1(Elastic)
40.00	26.67	0.10	0.03	120.00	0.61	CASE 1(Elastic)
50.00	33.33	0.13	0.04	150.00	0.76	CASE 1(Elastic)
60.00	40.00	0.15	0.05	180.00	0.91	CASE 1(Elastic)
70.00	46.67	0.18	0.06	197.62	1.07	CASE 2(Soil yield from upper)
80.00	53.33	0.20	0.07	197.62	1.29	CASE 2(Soil yield from upper)
90.00	60.00	0.23	0.08	197.62	1.63	CASE 3(Yield from bottom)
100.00	66.67	0.25	0.08	197.62	2.38	CASE 3(Yield from bottom)
109.34	72.89	0.28	0.09	197.62	20.06	CASE 3(Yield from bottom)
116	77.00	0.29	0.10	197.62	#NUM!	Unrealistic value
120	80.00	0.30	0.10	197.62	#NUM!	Unrealistic value
157	104.38	0.40	0.13	197.62	#NUM!	Unrealistic value
180	120	0.46	0.15	197.62	#NUM!	Unrealistic value
197.62	131.748	0.50	0.17	197.62	#NUM!	Unrealistic value

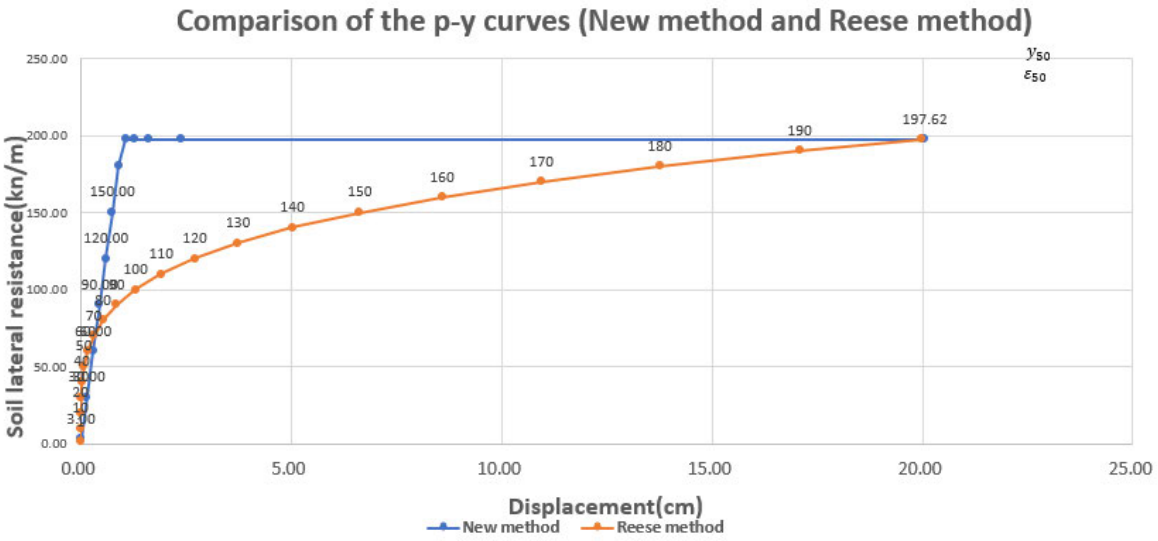

Figure 36: The p-y curve for S=2m, D=0.5m, and strength=50kPa

Table 14: The spreadsheet for S=1m, D=0.5m, and strength=100kPa

Lateral load(kN)	Moment(kN*M)	h	m	Soil lateral resistance(kN/m)	Normalised displacement	
		H/Plim/L	M/Plim/L			
1.00	0.67	0.00	0.00	3.00	0.01	CASE 1(Elastic)
10.00	6.67	0.02	0.01	30.00	0.11	CASE 1(Elastic)
20.00	13.33	0.04	0.01	60.00	0.22	CASE 1(Elastic)
30.00	20.00	0.06	0.02	90.00	0.33	CASE 1(Elastic)
40.00	26.67	0.07	0.02	120.00	0.44	CASE 1(Elastic)
50.00	33.33	0.09	0.03	150.00	0.55	CASE 1(Elastic)
60.00	40.00	0.11	0.04	180.00	0.66	CASE 1(Elastic)
70.00	46.67	0.13	0.04	210.00	0.78	CASE 1(Elastic)
80.00	53.33	0.15	0.05	240.00	0.89	CASE 1(Elastic)
90.00	60.00	0.17	0.06	270.89	1.00	CASE 1(Elastic)
100.00	66.67	0.18	0.06	270.89	1.11	CASE 1(Elastic)
110.00	73.33	0.20	0.07	270.89	1.29	CASE 2(Soil yield from upper)
130.00	86.67	0.24	0.08	270.89	1.90	CASE 3(Yield from bottom)
149.88	99.92	0.28	0.09	270.89	20.05	CASE 3(Yield from bottom)
180.00	120.00	0.33	0.11	270.89	#NUM!	Unrealistic value
200.00	133.33	0.37	0.12	270.89	#NUM!	Unrealistic value
220.00	146.67	0.41	0.14	270.89	#NUM!	Unrealistic value
240.00	160.00	0.44	0.15	270.89	#NUM!	Unrealistic value
246.95	164.63	0.46	0.15	270.89	#NUM!	Unrealistic value
250.00	166.67	0.46	0.15	270.89	#NUM!	Unrealistic value
270.89	180.59	0.50	0.17	270.89	#NUM!	Unrealistic value

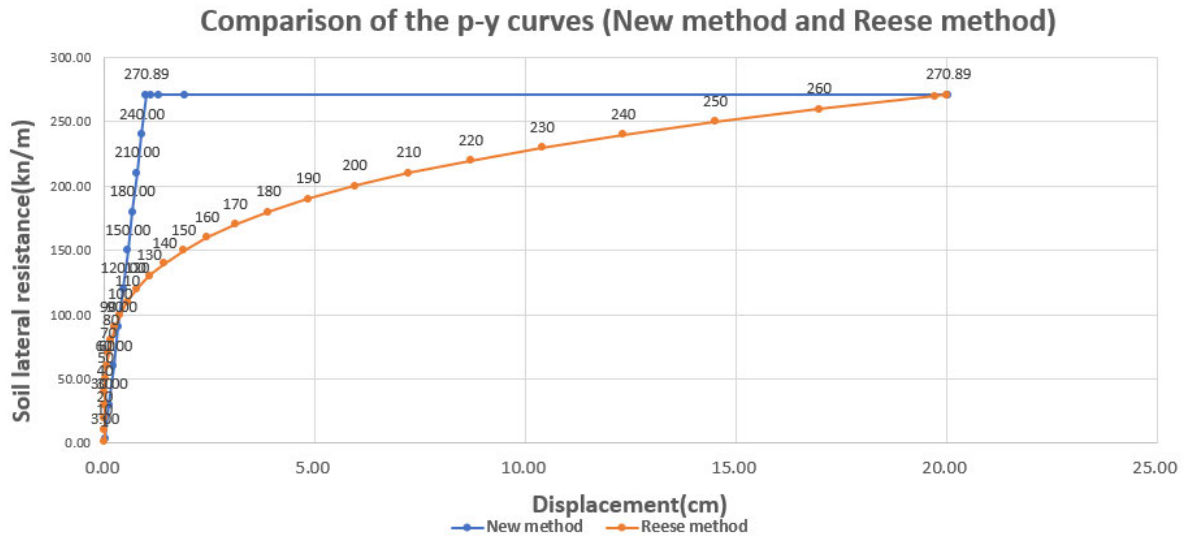

Figure 37: The p-y curve for S=1m, D=0.5m, and strength=100kPa

Table 15: The spreadsheet for S=2m, D=0.5m, and strength=100kPa

Lateral load(kN)	Moment(kN*M)	h	m	Soil lateral resistance(kN/m)	Normalised displacement	
		H/Plim/L	M/Plim/L			
1.00	0.67	0.00	0.00	3.00	0.01	CASE 1
10.00	6.67	0.01	0.00	30.00	0.08	CASE 1
20.00	13.33	0.03	0.01	60.00	0.16	CASE 1
30.00	20.00	0.04	0.01	90.00	0.24	CASE 1
40.00	26.67	0.05	0.02	120.00	0.32	CASE 1
50.00	33.33	0.07	0.02	150.00	0.39	CASE 1
60.00	40.00	0.08	0.03	180.00	0.47	CASE 1
70.00	46.67	0.09	0.03	210.00	0.55	CASE 1
80.00	53.33	0.11	0.04	240.00	0.63	CASE 1
90.00	60.00	0.12	0.04	270.00	0.71	CASE 1
100.00	66.67	0.13	0.04	300.00	0.79	CASE 1
110.00	73.33	0.14	0.05	330.00	0.87	CASE 1
120.00	80.00	0.16	0.05	360.00	0.95	CASE 1
150.00	100.00	0.20	0.07	380.75	1.23	CASE 2
180.00	120.00	0.24	0.08	380.75	1.81	CASE 3
210.66	140.44	0.28	0.09	380.75	20.00	CASE 3
220.00	146.67	0.29	0.10		#NUM!	Unrealistic state
240.00	160.00	0.32	0.11		#NUM!	Unrealistic state
260.00	173.33	0.34	0.11		#NUM!	Unrealistic state
280.00	186.67	0.37	0.12		#NUM!	Unrealistic state
300.00	200.00	0.39	0.13		#NUM!	Unrealistic state
320.00	213.33	0.42	0.14		#NUM!	Unrealistic state
340.00	226.67	0.45	0.15		#NUM!	Unrealistic state
360.00	240.00	0.47	0.16		#NUM!	Unrealistic state
380.75	253.83	0.50	0.17		#NUM!	Unrealistic state

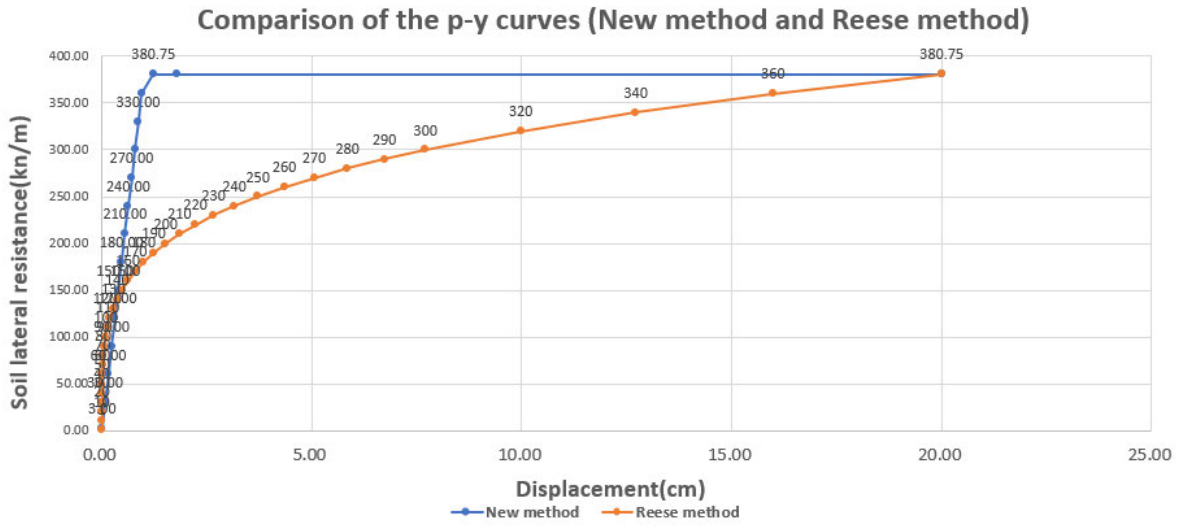

Figure 38: The p-y curve for S=2m, D=0.5m, and strength=100kPa

Table 16: The spreadsheet for S=1m, D=0.5m, and strength=200kPa

Lateral load(kN)	Moment(kN*m)	h	m	Soil lateral resistance(kN/m)	Normalised displacement	
		H/Plim/L	M/Plim/L			
1.00	0.67	0.00	0.00	3.00	0.01	CASE 1
10.00	6.67	0.01	0.00	30.00	0.06	CASE 1
20.00	13.33	0.02	0.01	60.00	0.12	CASE 1
30.00	20.00	0.03	0.01	90.00	0.17	CASE 1
40.00	26.67	0.04	0.01	120.00	0.23	CASE 1
50.00	33.33	0.05	0.02	150.00	0.29	CASE 1
60.00	40.00	0.06	0.02	180.00	0.35	CASE 1
70.00	46.67	0.07	0.02	210.00	0.40	CASE 1
80.00	53.33	0.08	0.03	240.00	0.46	CASE 1
90.00	60.00	0.09	0.03	270.00	0.52	CASE 1
100.00	66.67	0.10	0.03	300.00	0.58	CASE 1
110.00	73.33	0.11	0.04	330.00	0.63	CASE 1
120.00	80.00	0.12	0.04	360.00	0.69	CASE 1
150.00	100.00	0.14	0.05	450.00	0.86	CASE 1
180.00	120.00	0.17	0.06	521.13	1.04	CASE 2
210.00	140.00	0.20	0.07	521.13	1.21	CASE 2
250.00	166.67	0.24	0.08	521.13	1.87	CASE 3
280.00	186.67	0.27	0.09	521.13	2.81	CASE 3
288.33	192.22	0.28	0.09	521.13	20.08	CASE 3
330.00	220.00	0.32	0.11		#NUM!	Unrealistic state
360.00	240.00	0.35	0.12		#NUM!	Unrealistic state
390.00	260.00	0.37	0.12		#NUM!	Unrealistic state
410.00	273.33	0.39	0.13		#NUM!	Unrealistic state
430.00	286.67	0.41	0.14		#NUM!	Unrealistic state
450.00	300.00	0.43	0.14		#NUM!	Unrealistic state
480.00	320.00	0.46	0.15		#NUM!	Unrealistic state
510.00	340.00	0.49	0.16		#NUM!	Unrealistic state
521.13	347.42	0.50	0.17		#NUM!	Unrealistic state

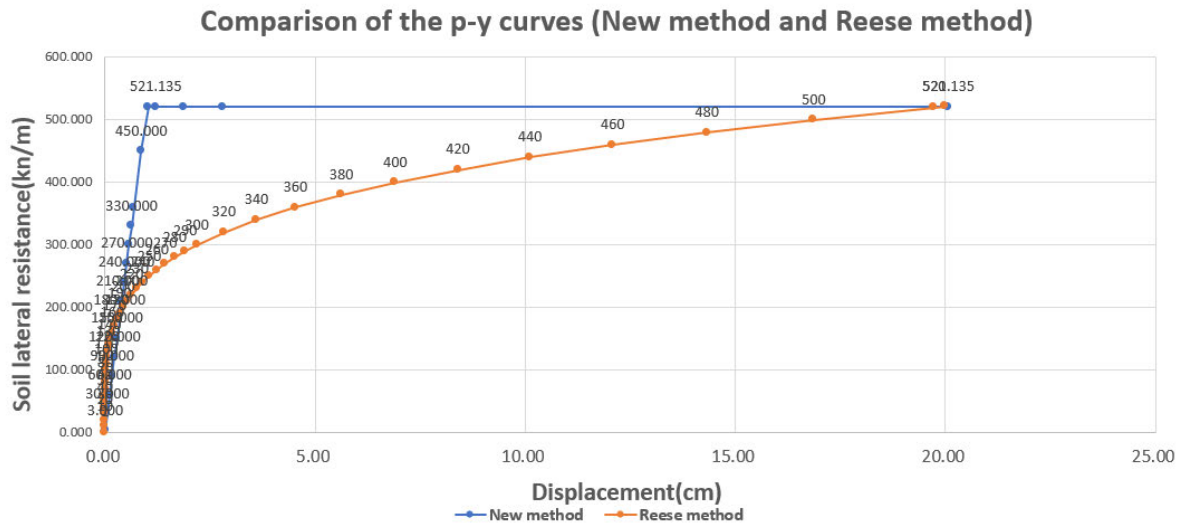

Figure 39: The p-y curve for S=1m, D=0.5m, and strength=200kPa

Table 17: The spreadsheet for S=2m, D=0.5m, and strength=200kPa

Lateral load(kN)	Moment(kN*m)	h	m	Soil lateral resistance(kN/m)	Normalised displacement	
		H/Plim/L	M/Plim/L			
1.00	0.67	0.00	0.00	3.00	0.00	CASE 1
10.00	6.67	0.01	0.00	30.00	0.04	CASE 1
20.00	13.33	0.01	0.00	60.00	0.08	CASE 1
30.00	20.00	0.02	0.01	90.00	0.12	CASE 1
40.00	26.67	0.03	0.01	120.00	0.16	CASE 1
50.00	33.33	0.03	0.01	150.00	0.20	CASE 1
60.00	40.00	0.04	0.01	180.00	0.24	CASE 1
70.00	46.67	0.05	0.02	210.00	0.28	CASE 1
80.00	53.33	0.05	0.02	240.00	0.32	CASE 1
90.00	60.00	0.06	0.02	270.00	0.37	CASE 1
100.00	66.67	0.07	0.02	300.00	0.41	CASE 1
110.00	73.33	0.07	0.02	330.00	0.45	CASE 1
120.00	80.00	0.08	0.03	360.00	0.49	CASE 1
130.00	86.67	0.09	0.03	390.00	0.53	CASE 1
150.00	100.00	0.10	0.03	450.00	0.61	CASE 1
180.00	120.00	0.12	0.04	540.00	0.73	CASE 1
210.00	140.00	0.14	0.05	630.00	0.85	CASE 1
240.00	160.00	0.16	0.05	720.00	0.97	CASE 1
260.00	173.33	0.18	0.06	739.03	1.06	CASE 2
280.00	186.67	0.19	0.06	739.03	1.16	CASE 2
300.00	200.00	0.20	0.07	739.03	1.29	CASE 2
350.00	233.33	0.24	0.08	739.03	1.82	CASE 3
408.89	272.59	0.28	0.09	739.03	20.01	CASE 3
410.00	273.33	0.28	0.09		#NUM!	Unrealistic state
430.00	286.67	0.29	0.10		#NUM!	Unrealistic state
441.08	294.05	0.30	0.10		#NUM!	Unrealistic state
450.00	300.00	0.30	0.10		#NUM!	Unrealistic state
500.00	333.33	0.34	0.11		#NUM!	Unrealistic state
550.00	366.67	0.37	0.12		#NUM!	Unrealistic state
570.00	380.00	0.39	0.13		#NUM!	Unrealistic state
600.00	400.00	0.41	0.14		#NUM!	Unrealistic state
620.00	413.33	0.42	0.14		#NUM!	Unrealistic state
650.00	433.33	0.44	0.15		#NUM!	Unrealistic state
680.00	453.33	0.46	0.15		#NUM!	Unrealistic state
700.00	466.67	0.47	0.16		#NUM!	Unrealistic state
739.03	492.69	0.50	0.17		#NUM!	Unrealistic state

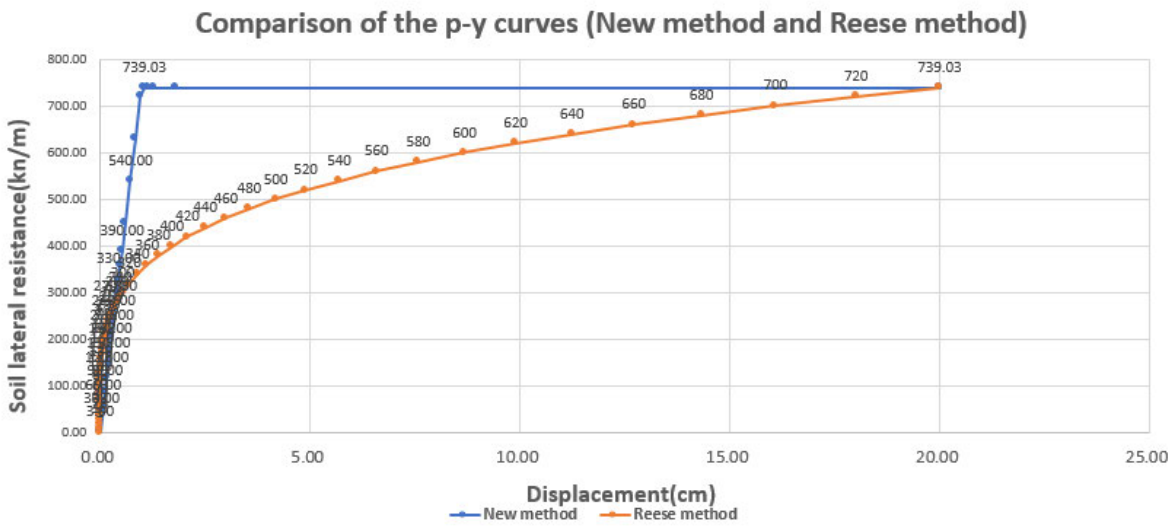

Figure 40: The p-y curve for S=2m, D=0.5m, and strength=200kPa

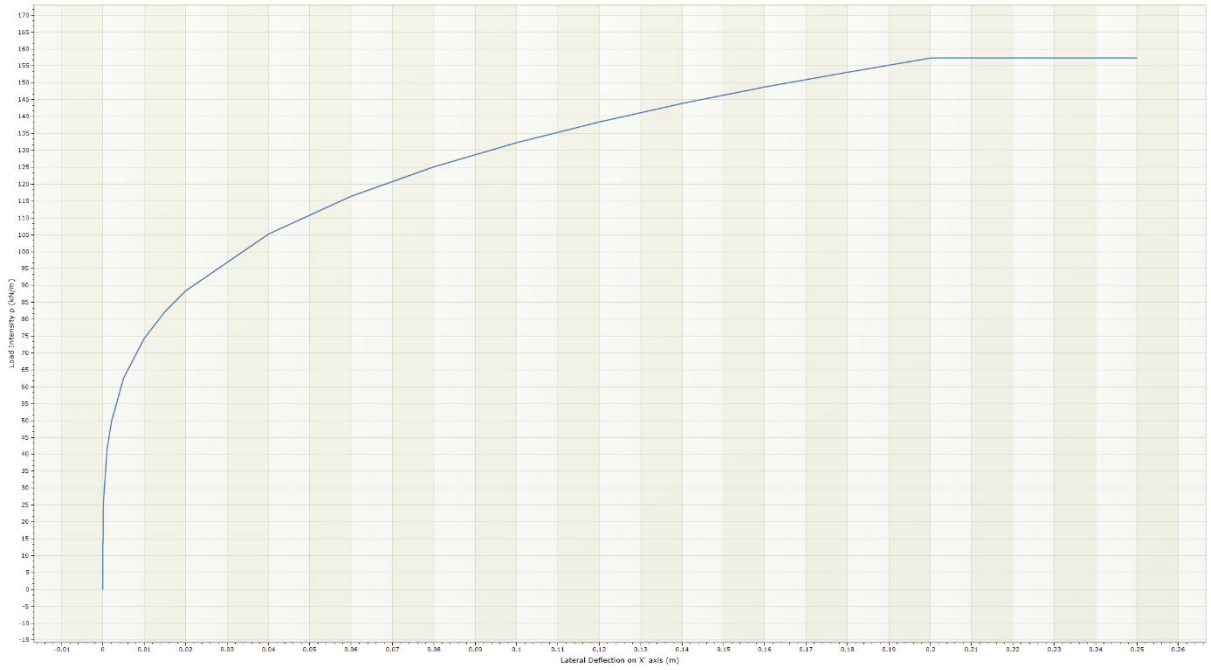

Figure 41: The p-y curve from RSPile (S=1m, D=0.5m, and strength=50kPa)

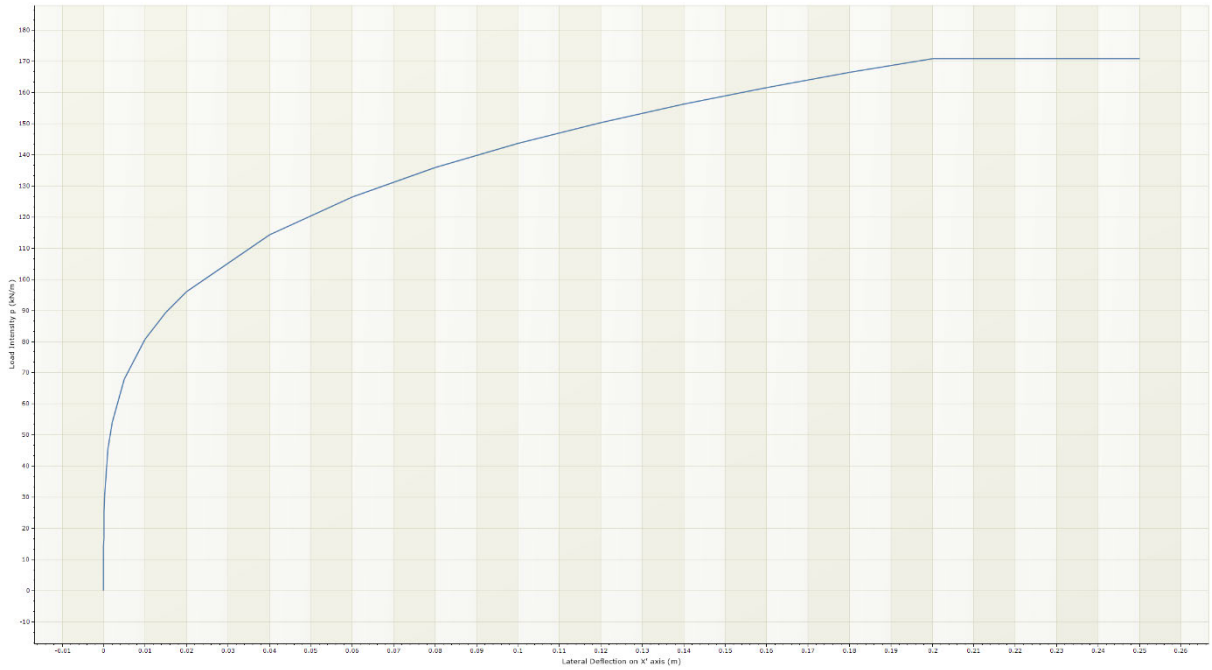

Figure 42: The p-y curve from RSPile (S=2m, D=0.5m, and strength=50kPa)

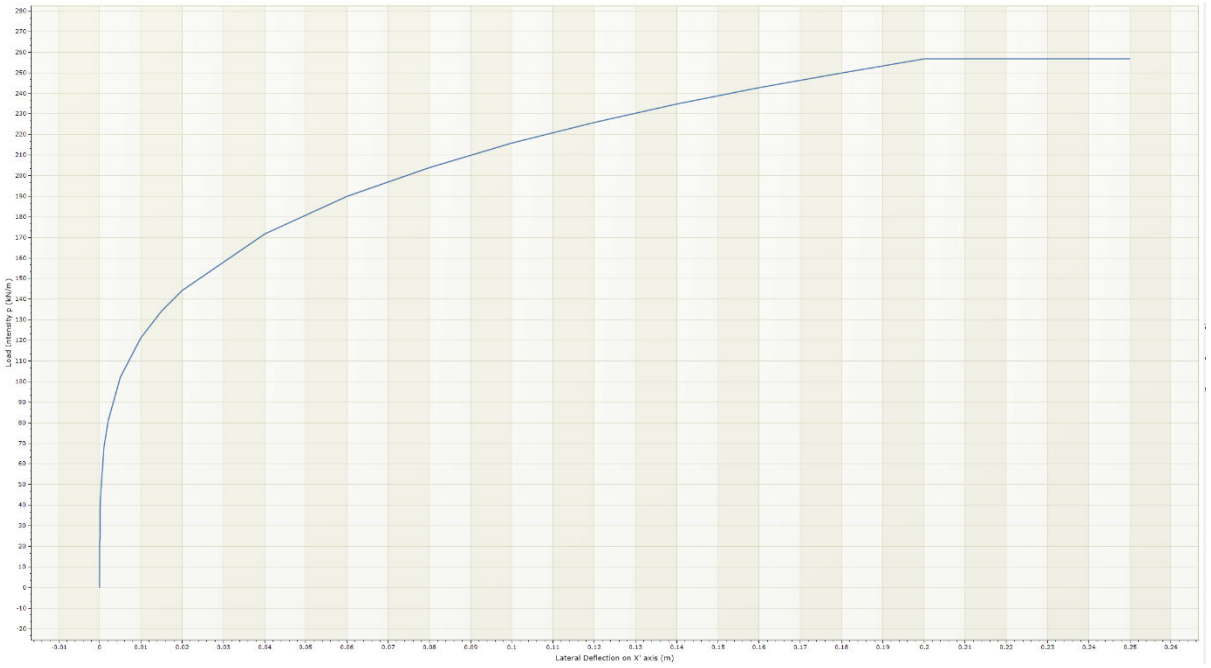

Figure 43: The p-y curve form RSPile (S=1m, D=0.5m, and strength=100kPa)

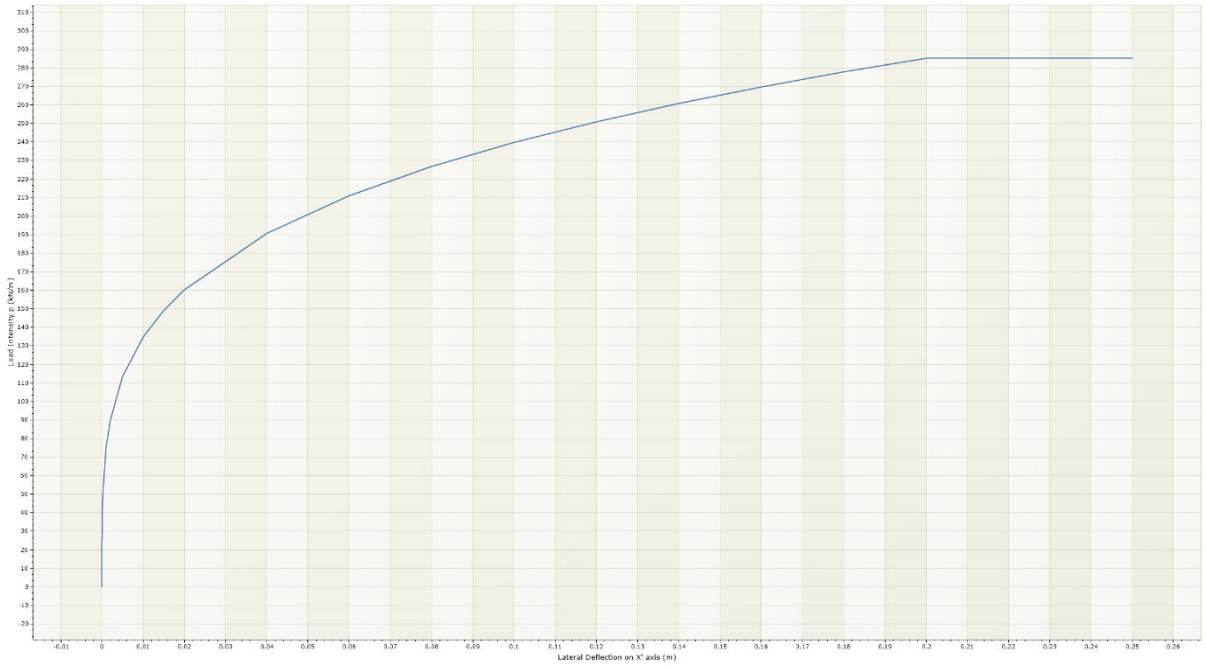

Figure 44: The p-y curve from RSPile (S=2m, D=0.5m, and strength=100kPa)

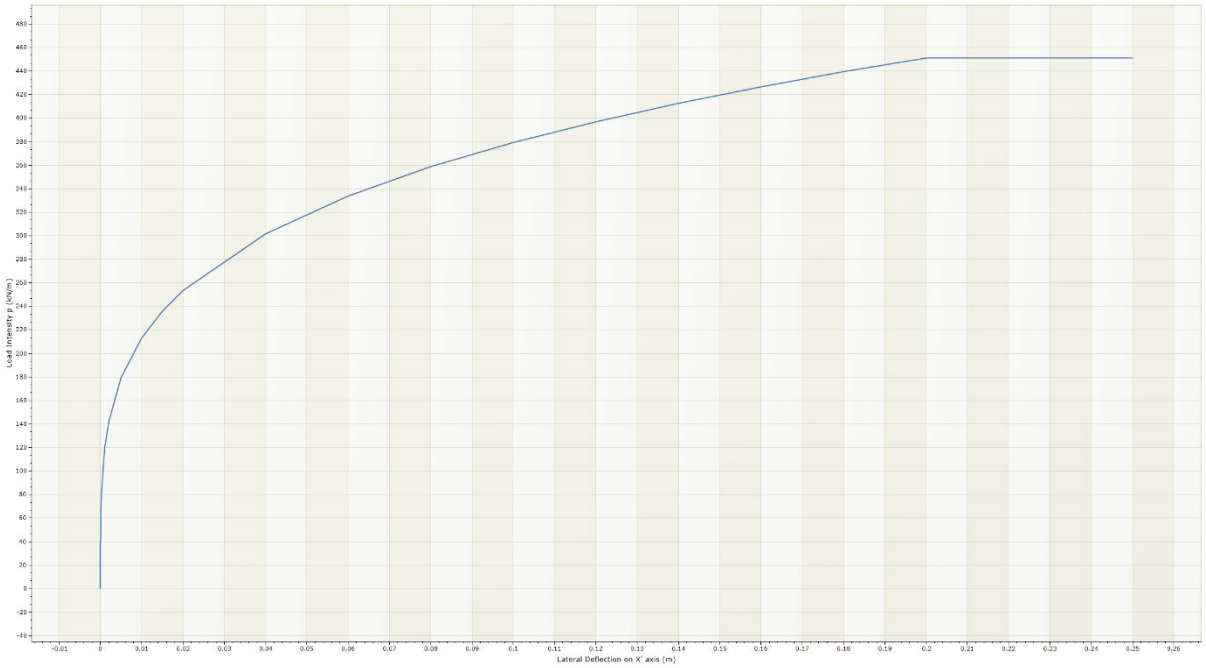

Figure 45: The p-y curve from RSPile (S=1m, D=0.5m, and strength=200kPa)

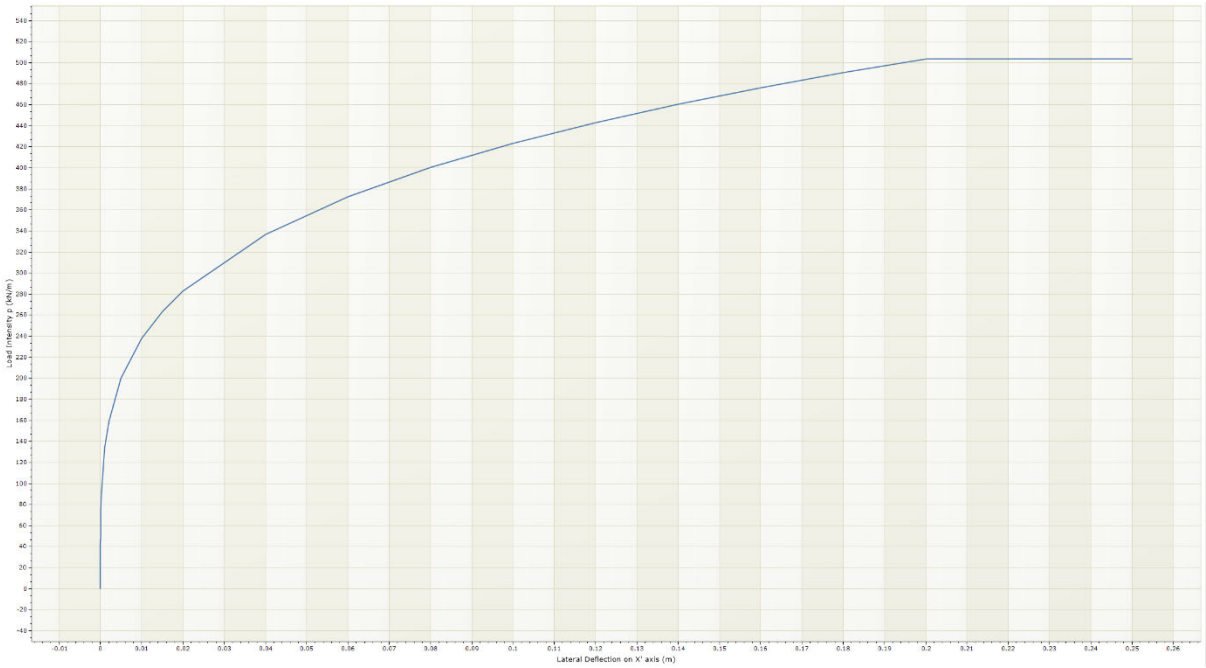

Figure 46: The p-y curve from RSPile (S=2m, D=0.5m, and strength=200kPa)